



HAL
open science

Experimental Demonstration of the Carbamazepine Crystallization from Non-photochemical Laser-Induced Nucleation in Acetonitrile and Methanol

Aziza Ikni, Bertrand Clair, Philippe Scoufflaire, S. Veessler, J.M. Gillet, Nouha El Hassan, Françoise Dumas, A. Spasojević-de Biré

► **To cite this version:**

Aziza Ikni, Bertrand Clair, Philippe Scoufflaire, S. Veessler, J.M. Gillet, et al.. Experimental Demonstration of the Carbamazepine Crystallization from Non-photochemical Laser-Induced Nucleation in Acetonitrile and Methanol. *Crystal Growth & Design*, 2014, 14 (7), pp.3286-3299. 10.1021/cg500163c . hal-01053346

HAL Id: hal-01053346

<https://hal.science/hal-01053346v1>

Submitted on 23 Sep 2020

HAL is a multi-disciplinary open access archive for the deposit and dissemination of scientific research documents, whether they are published or not. The documents may come from teaching and research institutions in France or abroad, or from public or private research centers.

L'archive ouverte pluridisciplinaire **HAL**, est destinée au dépôt et à la diffusion de documents scientifiques de niveau recherche, publiés ou non, émanant des établissements d'enseignement et de recherche français ou étrangers, des laboratoires publics ou privés.

This document is confidential and is proprietary to the American Chemical Society and its authors. Do not copy or disclose without written permission. If you have received this item in error, notify the sender and delete all copies.

**Experimental demonstration of the carbamazepine
crystallization from Non-Photochemical LASER-Induced
Nucleation in acetonitrile and methanol**

Journal:	<i>Crystal Growth & Design</i>
Manuscript ID:	Draft
Manuscript Type:	Article
Date Submitted by the Author:	n/a
Complete List of Authors:	Ikni, Aziza; Ecole Centrale Paris, Laboratoire Structures, Propriétés et Modélisation des Solides (SPMS), UMR CNRS 8580 Clair, Bertrand; Ecole Centrale Paris, Laboratoire Structures, Propriétés et Modélisation des Solides (SPMS), UMR CNRS 8580 Scouflaire, Philippe; Ecole Centrale Paris, Laboratoire "Energétique Moléculaire et Macroscopique, Combustion" (EM2C) UPR 288 Veesler, Stephane; CNRS, CINAM Gillet, Jean-Michel; Ecole Centrale Paris, Laboratoire Structures, Propriétés et Modélisation des Solides (SPMS), UMR CNRS 8580 El Hassan, Nouha; Ecole Centrale Paris, Laboratoire Structures, Propriétés et Modélisation des Solides (SPMS), UMR CNRS 8580 Dumas, Françoise; CNRS, Université Paris Sud, BioCIS Spasojevic - de Biré, Anne; Ecole Centrale Paris, Laboratoire Structures, Propriétés et Modélisation des Solides (SPMS), UMR CNRS 8580

SCHOLARONE™
Manuscripts

1
2
3
4
5
6
7
8
9
10
11
12
13
14
15
16
17
18
19
20
21
22
23
24
25
26
27
28
29
30
31
32
33
34
35
36
37
38
39
40
41
42
43
44
45
46
47
48
49
50
51
52
53
54
55
56
57
58
59
60

Experimental demonstration of the carbamazepine crystallization from Non-Photochemical LASER- Induced Nucleation in acetonitrile and methanol

*Aziza Ikni^{1,2}, Bertrand Clair^{1,2}, Philippe Scouflaire^{1,3}, Stéphane Veesler⁴, Jean-Michel
Gillet^{1,2}, Nouha El Hassan^{1,2}, Françoise Dumas⁵, Anne Spasojević-de Biré^{1,2*}*

¹ Ecole Centrale Paris, Grande Voie des Vignes, 92295 Châtenay-Malabry, France

² CNRS, UMR 8580, Laboratory “Structures Propriétés et Modélisation des Solides” (SPMS), Grande
Voie des Vignes, 92295 Châtenay-Malabry, France

³ CNRS, UPR 288, Laboratory “Energétique Moléculaire et Macroscopique, Combustion” (EM2C),
Grande Voie des Vignes, 92295 Châtenay-Malabry, France

⁴ CNRS , UMR 7325, Laboratory “Centre Interdisciplinaire de Nanoscience de Marseille”
(CINaM), Campus de Luminy, Case 913, 13288 Marseille, France

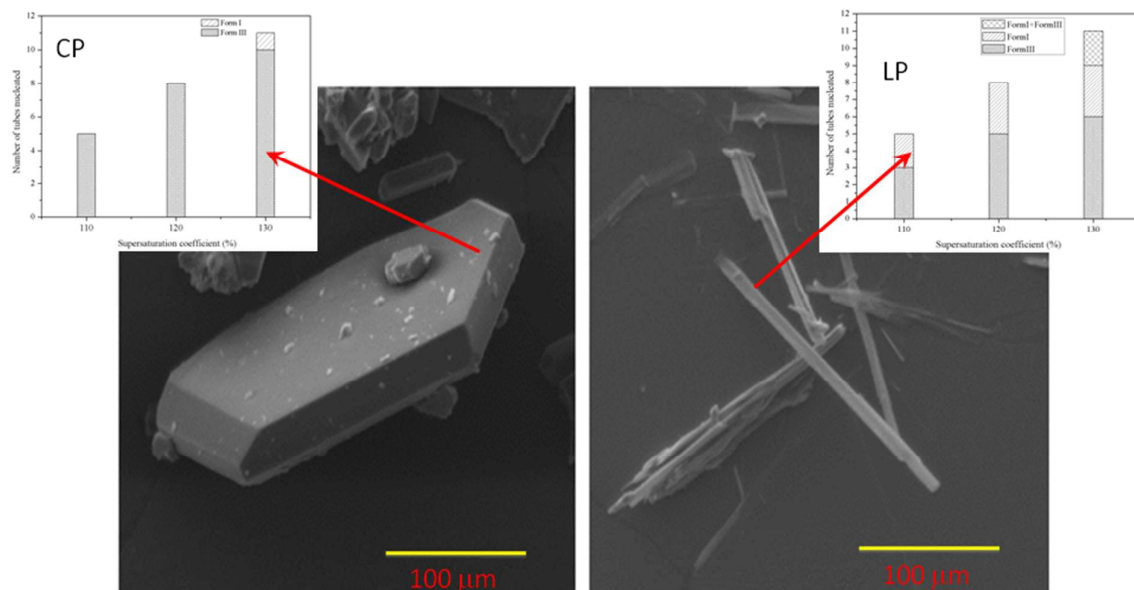
⁵ CNRS, UMR 8076, Laboratory BIOCIS, Faculté de Pharmacie, Université Paris-Sud, 5, rue
Jean-Baptiste Clément, 92296 Châtenay-Malabry, France

To be submitted Crystal Growth and Design

1
2
3 Abstract
4
5
6
7
8
9
10
11
12
13
14
15
16
17
18
19
20
21
22
23
24
25
26
27
28
29
30
31
32
33
34
35
36
37
38
39
40
41
42
43
44
45
46
47
48
49
50
51
52
53
54
55
56
57
58
59
60

The paper reports for the first time the crystallization of Carbamazepine (CBZ) molecule in two solvents (methanol, acetonitrile) using Non-Photochemical LASER-Induced Nucleation (NPLIN) technique. The metastable zone of CBZ is first determined experimentally for different temperatures in both solvents. Then, the prepared solutions are irradiated by a 532nm wavelength nano-second pulsed LASER and permitted to obtain CBZ crystals of forms I and III. The impact of LASER power and polarization (circular (CP) and linear (LP)) on the CBZ crystallization efficiency in both solvents is carried-out through experiments. According to the results, the crystallization efficiency is significantly higher in methanol than in acetonitrile and it is higher in solutions irradiated by CP LASER than LP LASER. Moreover, the irradiation of acetonitrile solution by a LP LASER results in CBZ form I and III, whereas CP LASER leads to CBZ form III crystals. An *ab initio* determination of the energy interaction of different pairs of CBZ has been carried-out that enables the explanation of the nucleation in acetonitrile for both polarizations. In methanol, only CBZ form III is obtained which is in agreement with the possibility of methanol to create non-covalent interactions preventing the CBZ form I and II nucleation.

Graphical abstract



1
2
3
4
5
6
7
8
9
10
11
12
13
14
15
16
17
18
19
20
21
22
23
24
25
26
27
28
29
30
31
32
33
34
35
36
37
38
39
40
41
42
43
44
45
46
47
48
49
50
51
52
53
54
55
56
57
58
59
60

I- Introduction

Crystallization is an important separation and purification process employed to produce a wide variety of materials in industries. Crystallization plays a vital role in the pharmaceutical industry since it is a process that is used during final and intermediate stages of the manufacturing process of Active Pharmaceutical Ingredients (APIs). The operating conditions of the crystallization process determine the physical properties of the APIs such as the crystal purity, phase, shape, and size distribution. Moreover, these properties determine the efficiency of downstream operations, such as filtration, drying and formulation, and the product effectiveness, such as bioavailability and shelf-life. For pharmaceutical APIs that exhibit various phases or stereoisomers, the crystallization process also affects the phase produced and the extent of chiral separation.¹ Indeed, different phases of a drug substance can have different chemical and physical properties. These properties can affect the ability to process and/or manufacture the drug substance and the drug product, as well as on drug product stability, dissolution, and bioavailability. Therefore, polymorphism can affect the quality, safety, and efficacy of the drug product.²⁻⁶ Many examples are reported in literature, see for instance the report on Ritonavir[®] and Rotigotine[®].⁶ These works highlight the importance of polymorphism study during the process of manufacturing of drugs. All these examples clearly show that it is highly important to make the required polymorphic form, as the other form may not show the desired effects. Therefore, polymorphism control is an important step. Within this context, the work carried-out in this paper aims at demonstrating experimentally the crystallization of active pharmaceutical ingredients (APIs) using the Non-Photochemical LASER-Induced Nucleation (NPLIN) technique.⁷ The carbamazepine (C₁₅H₁₂N₂O, CBZ) molecule (figure 1a) was selected mainly because, in pharmaceutical research, it has been extensively studied as a model compound for solid-form discovery and control since it is known to form four different anhydrous phases (or 4 different polymorphs). The complete list

1
2
3 of references, with the different nomenclature of these four CBZ polymorphs is reported by
4
5 Grzesiak *et al.*⁸ The lattice data for the four crystallographic forms are summarized in table
6
7 S1 provided as supplementary materials. In addition to these four polymorphic forms, more
8
9 than 60 solvates, hydrates and co-crystals, have been identified and characterized.⁹⁻¹⁰
10
11 According to experimental⁸ and computational results⁹ the theoretical stability order of the
12
13 four polymorphs at ambient temperature and at 0 K is form III > form I > form IV > form II.
14
15 The commercially available form is the form III. It can be crystallized from various solvents
16
17 with high dielectric constants.
18
19

20
21 This paper begins by a bibliographical description of the works reported in literature and
22
23 that deal with the crystallization mainly based on the NPLIN technique. It presents the
24
25 possibility of obtaining CBZ crystals in methanol and acetonitrile using NPLIN technique.
26
27 We show that CBZ nucleation is launched and controlled by the LASER power in the
28
29 metastable zone and define the experimental conditions to produce CBZ crystals of good
30
31 quality. We measure the CBZ metastable zone in methanol and acetonitrile at different
32
33 temperatures: 5°C, 20°C, 30°C and 40°C. The solutions are irradiated by a 532 nm
34
35 wavelength LASER. Moreover, different LASER power values and polarizations, linear and
36
37 circular, are used to study the impact of LASER on crystallization efficiency as well as on
38
39 polymorphic form. Finally, an *ab initio* determination of the energy interaction of different
40
41 pairs of CBZ are performed in order to understand the behavior of the nucleation in
42
43 acetonitrile within the two polarizations.
44
45
46
47
48

49 **II- Brief bibliographic survey of unusual polymorphism and nucleation control techniques**

50
51 Research on polymorphism and material properties of active drug compounds is an integral
52
53 part of drug development. In this paper, we will not discuss the usual approach consisting in
54
55 studying the effect of the solute concentration, temperature, medium of crystallization and
56
57
58
59
60

1
2
3 hydrodynamics on the crystallization and polymorphism^{2, 11}, but we will focus on
4
5 crystallization experiments based on the use of a LASER as an external field. It should be
6
7 noted that other external fields were also reported in the literature such as ultrasound¹²⁻¹⁴,
8
9 magnetic field and electric field¹⁵⁻¹⁸, etc. The main objective of using external fields is the
10
11 nucleation control.¹⁹ The impact of an externally applied field on the crystal growth in
12
13 solutions were highlighted by Voss²⁰ and Oxtoby.²¹ This field influences nucleation, through
14
15 molecular orientation, as well as density fluctuation. The most documented technique is the
16
17 light induced nucleation technique that can be subdivided into two categories: The
18
19 Photochemical Light-Induced Nucleation (PLIN) and the Non Photochemical LASER-
20
21 Induced Nucleation (NPLIN). In PLIN experiments, the light has sufficient energy to cause
22
23 ionization or to create radicals that subsequently react to produce nucleation centers²²,
24
25 whereas in the NPLIN experiments the LASER is at wavelength in the non-absorbing zone of
26
27 the solute molecule.⁷ In the following, we will give an overview of the works reported in
28
29 literature for both categories.
30
31
32

33 **Photochemical Light-Induced Nucleation**

34
35
36 PLIN technique is a nucleation process, which is accompanied by a chemical reaction
37
38 induced by light. This was first reported in solution by Tyndall²³ and then in the vapor phase
39
40 as LASER snow.²⁰ Then, many papers were reported in the literature as detailed in this
41
42 section. Indeed, Okutsu *et al.*²¹ found an effect of LASER radiation on the nucleation of
43
44 benzophenone in ethanol/water mixed solution. The irradiation of supersaturated solutions
45
46 results in the formation benzopinacol precipitants, which is related to photochemistry
47
48 phenomena. The obtained crystal was composed of benzopinacol produced from excited
49
50 benzophenone through a benzophenone ketyl radical. Later, Okutsu *et al.*²⁴ showed that the
51
52 irradiation of a metastable supersaturated lysozyme solutions by a Xenon lamp induce
53
54 nucleation. It was observed that irradiation of lysozyme molecules in solution enhances the
55
56
57
58
59
60

1
2
3 attractive interaction between molecules in solution. They also observed that there is an
4
5 irradiation time beyond which the protein is denatured. Veessler *et al.*²⁵ proposed seeding non-
6
7 irradiated solutions of lysozyme with limited amounts of irradiated lysozyme solution, in
8
9 order to avoid denaturation of protein by excessive irradiation. Moreover, it was demonstrated
10
11 by absorption experiments that the irradiation of lysozyme²⁵, thaumatin²⁶ and Ribonuclease²⁷
12
13 produces photochemical intermediate, neutral radicals, which enhance nucleation.
14
15

16
17 However, the fact that the PLIN involves a chemical reaction and a formation of radicals
18
19 could be non-desirable in some cases. This limitation can be overcome through the use of the
20
21 NPLIN technique as explained hereafter.
22

23 **Non-Photochemical LASER-Induced Nucleation**

24
25 In this case, the LASER wavelength is chosen, in order not to be absorbed by the solution
26
27 and therefore the nucleation is not accompanied by a photochemical reaction. The NPLIN was
28
29 first observed by Tam *et al.*²⁸ They worked on vapors of Cesium with small amount of
30
31 hydrogen, and observed that upon irradiation by a LASER, some particles appeared, which
32
33 they identified as cesium-hybrid crystals. More recently Garetz *et al.*^{29, 30} have reported
34
35 experimental results showing that polymorphism control can be achieved through NPLIN.
36
37 The first experiments were done with supersaturated urea solutions.⁷ From the analysis of the
38
39 obtained results, they suggested that the optical Kerr effect was responsible for the alignment
40
41 of molecules due to the electric field. Since then, extensive research works were carried-out in
42
43 this area and numerous papers were reported in literature as summarized on table 1. Some of
44
45 these papers do not use the NPLIN term for defining their experiments. In this paper, we use
46
47 the acronym NPLIN for all the experiments in which a supersaturated solution irradiated
48
49 using LASER results in the formation of a crystalline compound without change of its
50
51 chemical formula.
52
53
54
55
56
57
58
59
60

1
2
3 These works can be decomposed into four main categories: small organic molecules,
4 inorganic molecules, protein molecules and miscellaneous. These categories are briefly
5 described hereafter. For all these categories, the LASER employed to enhance nucleation is
6 either of pulsed or continuous type and could be focalized or not. In the case of pulsed type
7 LASER, the LASER pulse duration is either of the nano-second range, femto-second or pico-
8 second range. An analysis of the experimental setups used in these experiments has been
9 described by Clair *et al.*³¹

18 ***Small organic molecules***

19
20 Glycine^{29-30,32-36}, urea^{7,37}, L-histidine³⁸, 4-(dimethylamino)-*N*-methyl-4-stilbazolium
21 tosylate (DAST)^{39,40} and glacial acetic acid⁴¹ molecules have been crystallized through
22 NPLIN method.
23
24
25

26
27 Garetz *et al.*³⁰ demonstrated experimentally the nucleation of glycine in aqueous
28 supersaturated solutions using nano second unfocalized pulsed LASER. The paper reports that
29 the control of polymorphism of glycine was achieved through the control of laser polarization
30 (linear polarization (LP) or circular polarization (CP)) in a specific range (1.46 - 1.55) of
31 supersaturated solution. According to their conclusions, the LP LASER results in γ
32 polymorph and the CP LASER leads to α polymorph, which is called switch window. The
33 interpretation provided for the nucleation is based on the reorientation of the molecules under
34 an intense electromagnetic field and the crystallization is triggered by optical Kerr effect.
35 Rungsimanon *et al.*³³ studied the crystallization of glycine in unsaturated heavy water solution
36 by irradiating the solution with a LP continuous and focalized LASER type at 1064 nm
37 wavelength. The obtained crystal is of γ form. The control mechanism was explained in terms
38 of a local variation of a supersaturation value induced by LASER trapping of the liquid-like
39 clusters and the subsequent temperature increase. According to the paper, this form cannot be
40 obtained by the classical crystallization techniques. Yuyama *et al.*³⁴ demonstrated that under
41
42
43
44
45
46
47
48
49
50
51
52
53
54
55
56
57
58
59
60

1
2
3 specific solution conditions: supersaturated or undersaturated or saturated and under specific
4
5 LASER polarization, it is possible to achieve a selective crystallization of α and γ polymorphs
6
7 of glycine. According to their results, supersaturated/saturated solutions irradiated by a low
8
9 power CP LASER enhances γ crystals formation while for unsaturated solution LP LASER at
10
11 a specific power (1.4 W) increases the probability of γ crystals formation. Recently Liu *et*
12
13 *al.*³⁶ have demonstrated a femtosecond LASER-induced crystallization of glycine in its
14
15 aqueous supersaturated solution. They found that crystals' morphology of prepared by
16
17 cavitations bubble formation upon the femto-second irradiation into solution depends on the
18
19 LASER repetition rate. Lower repetition rate of femto-second LASER irradiation tends to
20
21 result in single crystal formation. Moreover, they found an increase in crystallization
22
23 probability at air/solution interface, which means an important interplay between molecular
24
25 adsorption and spatial limitation of mechanical stress induced by bubble formation and then
26
27 cavitations. However, the authors did not give information about the obtained polymorphic
28
29 form.
30
31
32

33
34 Sun *et al.*³⁸ reported polarization switching of polymorphs in LASER irradiated L-histidine
35
36 supersaturated solutions in the range 1.4-1.6. CP laser leads to orthorhombic A polymorph,
37
38 whereas LP laser leads to a mixture of both orthorhombic A and orthorhombic B.
39

40
41 Regarding DAST, Hosokawa *et al.*⁴⁰ demonstrated experimentally the efficiency of
42
43 femtosecond LASER pulses on the crystallization of supersaturated methanol solutions of
44
45 DAST.
46

47 ***Small inorganic molecules***

48
49 The application of the NPLIN technique to the inorganic molecules has been demonstrated,
50
51 for the first time, by Alexander *et al.*⁴²⁻⁴⁵ on the crystallization of KCl. Later, other works
52
53 were reported in the literature concerning KBr⁴⁵, NaClO₃⁴⁶, KMnO₄ and (NH₄)₂SO₄⁴⁷ and
54
55 KNO₃.⁴⁸ According to Alexander *et al.*⁴² a single, 7 ns pulse of near-infrared (1064 nm)
56
57
58
59
60

1
2
3 LASER light is sufficient to grow a single crystal of supersaturated aqueous potassium
4
5 chloride in the range 1.05-1.10. Moreover, the nucleation is likely enhanced through the
6
7 isotropic electronic polarization of subcritical KCl clusters by LASER light and a decrease in
8
9 the free-energy surface on which a small proportion of the clusters become supercritical. The
10
11 work reported by Duffus *et al.*⁴³ on the same molecule in agarose gel permitted a spatial
12
13 control of crystal nucleation using NPLIN and demonstrated that the NPLIN efficiency
14
15 depends on the peak power density of the LASER pulse and not on the total energy delivered
16
17 to the solution. Ward *et al.*⁴⁵ studied the impact of both LASER wavelength as well as
18
19 temperature on the NPLIN of KCl and KBr from supersaturated aqueous solutions. They
20
21 reported that solutions irradiated with 532 nm pulses resulted in a lower threshold power to
22
23 nucleation than 1064 nm. Ward *et al.*⁴⁶ have also investigated NPLIN in molten sodium
24
25 chlorate (NaClO₃). They demonstrated a propensity towards nucleation of the same
26
27 enantiomorph (levorotatory or dextrorotatory) of the cubic phase that was used prior to
28
29 melting. The nucleation mechanism is most likely heterogeneous.
30
31
32

33 34 ***Proteins molecules***

35
36 Many experimental studies were reported in literature; the most studied protein is hen egg-
37
38 white lysozyme (HEWL). The first report of the NPLIN of proteins molecule was by Adachi
39
40 *et al.*⁴⁹ They used a focused femto-second laser pulses of 780 nm in order to induce
41
42 nucleation of HEWL. It was observed that the number of nucleated HEWL crystals strongly
43
44 depends on LASER irradiation conditions. Indeed, the generated crystals increased in number
45
46 as the irradiated LASER pulses number increased. The following reported works focused on
47
48 the nucleation of the same protein in an aqueous solution^{50,51,56} or in gel solution media.^{52-53,}
49
50
51
52
53
54
55
56
57
58
59
60
57 To study the nucleation of HEWL in a solution, Lee *et al.*⁵⁰ employed unfocalised nano
second and pico second pulsed LASER, instead of a focused femto second pulsed LASER.
They noticed that NPLIN in lysozyme solutions was more effective with shorter aging time,

1
2
3 532 nm wavelength, higher peak intensity, and shorter pulse duration. According to their
4
5 conclusions, the nucleation mechanism could be attributed to electric-field-induced
6
7 reorganization in conjunction with the increased concentration fluctuations. Tsuboi *et al.*⁵¹
8
9 demonstrated the nucleation of lysozyme in heavy water by photon pressure generated by a
10
11 continuous wavelength 1064 nm LASER beam during 1-2 h. They observed lysozyme
12
13 molecular aggregates. For the sake of understanding the nucleation mechanism of proteins,
14
15 the solution is replaced by a gel.⁵³ In free solution, when an external field is applied its effect
16
17 is counteracted by re-homogenizing the solution by convection; therefore different authors⁵³⁻⁵⁵
18
19 proposed the use of a gel medium (polyethylene glycol, PEG 6000 or agarose gel) to suppress
20
21 clusters, nuclei and crystals diffusion in crystallization experiments in presence of external
22
23 fields. According to Nakamura *et al.*⁵³ the femto-second laser-induced shockwave and
24
25 cavitation bubble generation processes are key factors for crystallization. Later, similar
26
27 experimental works⁵⁴⁻⁵⁸ confirmed the provided explanation for the nucleation mechanism in
28
29 these experimental conditions.
30
31
32

33 34 *Miscellaneous*

35
36 This category concerns NPLIN of liquid crystals or gas bubbles. For instance, Sun *et al.*⁶⁰
37
38 studied a single-component liquid crystalline phase transition in supercooled 40-n-pentyl-4-
39
40 cyanobiphenyl. According to their results, the nematic director showed a tendency to align
41
42 with the linear polarization vector of the LASER, and the authors concluded that the order is
43
44 transferred by enhancing fluctuations in the nematic phase in the direction of the electric field
45
46 of the LASER. Moreover Knott *et al.*⁶¹ demonstrated that laser pulses of similar duration,
47
48 intensity, and wavelengths can induce the nucleation of CO₂ bubbles in carbonated water.
49
50 They have shown that the threshold pulse energy to induce CO₂ decreases with increasing
51
52 solution supersaturation.
53
54
55
56
57
58
59
60

1
2
3 From the above overview, summarized in table 1, we can note that most of the reported
4 works have dealt with nucleation of molecules in aqueous supersaturated solutions. The work
5 presented in this paper addresses the nucleation of organic molecule in organic solvents.
6
7
8

9 10 11 **III- Material, method and experiments**

12 **III-1- Material**

13
14 Commercial carbamazepine (>99%, form III powder) was obtained from Enzo Life Sciences
15 company and stored at 4° C. Absolute methanol (>99,8%) and acetonitrile (>99.9%),
16 purchased from Merck (Darmstadt, Germany) were used as the crystallization solvents.
17
18
19

20 **III-2- LASER irradiation bench set-up and parameters**

21
22 An overview of the home-made set-up that we specially developed for the NPLIN
23 experiments is given in figure 2. An annular LASER light beam is generated by a Quanta-
24 ray®Q-switched Nd:YAG LASER, producing a 10 pulses *per* second train of linearly-
25 polarized 7-ns LASER pulses at 532 nm. The irradiation duration time control is achieved
26 using a shutter Thor Lab® (SC05 / SH 10). The reduction of the LASER beam diameter could
27 be done through two types of equipments a laboratory made telescope with a Nitrogen gas
28 circulation for avoiding plasma discharge at the focal point and a commercial condenser
29 (HEBX-3X from Melles Griot®). These equipments permit to reduce the beam size from 7 to
30 3.5 mm. The linearly polarized light is converted to circular polarization by sending it through
31 a Glan polarizer followed by a Quarter Wave plate. A mirror is employed to reflect the beam
32 by 90° in order to direct it towards the HPLC tube. The LASER power was measured both
33 right after the laser source by making use of a mirror that reflects a portion of the LASER
34 beam and its intensity measured using a Wattmeter (QE25LB-S-MB). More details on the
35 experimental set up can be found in Clair *et al.*³¹
36
37
38
39
40
41
42
43
44
45
46
47
48
49
50
51
52
53
54

55 After preparing the solutions in the tubes and then placing them on the thermostatic sample
56 holder by a circulating bath at 20°C, we adjust the different parameters of the LASER used to
57
58
59
60

1
2
3 irradiate the tubes. The sample holder is then set to rotation in order to irradiate the 90 tubes
4
5 one by one by the LASER beam. However, it should be noted that for the CP LASER, the
6
7 power intensity is limited to 0.35 GW/cm². Each tube is observed under an inverted
8
9 microscope, and microphotographs are taken using a CCD camera connected to the
10
11 microscope at regular time intervals in order to follow the evolution of the crystallization. The
12
13 different microphotographs were then digitally stored in a computer for further analysis.
14
15

16 **III-3- The CBZ metastable zone and spontaneous nucleation**

17
18 In order to demonstrate the impact of LASER radiation on the formation of crystals, it is
19
20 necessary to start by determining the CBZ metastable zone for a given solvent. The
21
22 potentiality to realize thermodynamically metastable states is a characteristic feature of the
23
24 first order phase transition.⁶² Starting from the initial phase, supersaturating the solution
25
26 during a time interval t_i leads to the formation of a new phase materialized by the appearance
27
28 of crystals. The time interval t_i separating these two phases is referred to as the induction time
29
30 and is used as a measure of the ability of the system to remain in a metastable equilibrium. It
31
32 can therefore be used to determine the metastability limit of the initial phase. Indeed, it allows
33
34 us to determine the critical supersaturation coefficient (β_c) below which the initial phase can
35
36 stay long enough without losing its metastability.
37
38
39

40
41 The determination of the metastable zone of the studied carbamazepine (form III) in
42
43 methanol and acetonitrile solutions follows the above-described procedure. To that end, the
44
45 experimental setup used for screening crystallization conditions and to investigate solution
46
47 mediated phases transitions of an active pharmaceutical ingredient is described by Detoisien
48
49 *et al.*¹¹ It is composed of multi-well setup (ANACRISMAT, France) that consists of a two
50
51 dimensional (X and Y) motorized stage mounted on a Nikon[®] (Eclipse TE2000-U) inverted
52
53 optical microscope used in conjunction with an adapted Peltier temperature control unit (± 0.1
54
55 °C). The motorized stage designed to carry two blocks of 12, 24 or 48 well according to the
56
57
58
59
60

1
2
3 vials used. We used standard HPLC glass vial (diameter 12 mm) with 1 ml of solvent in
4
5 which crystals of carbamazepine could be observed. Sequential image acquisitions are
6
7 performed automatically and periodically (from minutes to hours), by using a digital camera.
8

9
10 We carried-out a series of experiments that consist in preparing different solutions at
11
12 different supersaturation coefficients β , stored and observed at different temperatures (5°C,
13
14 20°C, 30°C and 40°C). The experimental conditions are summarized in Table 2. The
15
16 supersaturation coefficient β is defined by $(C/C_s*100\%)$, where C is the solution
17
18 concentration and C_s is the solubility at a given temperature ranging from 5 to 45°C.⁶³ The
19
20 observation of the nucleation in the different prepared solutions at different instants using
21
22 microscope allowed us to measure the time required for crystals to appear in each sample.
23
24 This time was noted as the induction time (t_i) for each sample. Consequently, we considered
25
26 the critical supersaturation coefficient β_c to be the concentration value under which the
27
28 solutions did not crystallize after a time sufficiently long enough t_i . The schematic illustration
29
30 of the method used to determine the metastable zone of CBZ with in situ microscopy is given
31
32 in Figure 3a. In order to study the spontaneous nucleation efficiency as function of
33
34 supersaturation, the solution observation is carried-out after the time duration t_i . The
35
36 supersaturation coefficient values are always chosen within the range of the values that were
37
38 used above and permitted to determine the metastable zone width.
39
40
41
42

43 **III-4- Supersaturated solutions preparation for NPLIN**

44

45
46 Four sets of experiments were performed using a total of 360 supersaturated solutions
47
48 irradiated with a LASER at 532 nm of linear and circular polarizations respectively. For each
49
50 set, three different concentrations were prepared. For each solution concentration, 30 identical
51
52 glass tubes were prepared at 20 °C. The 30 glass tubes were decomposed into three groups.
53
54 Each group of glass tubes is irradiated using different laser energies.
55
56
57
58
59
60

1
2
3 According to the results obtained in the previous section and the determination of the
4 critical supersaturation $\beta_{c,T,S}(t)$, the prepared supersaturated solutions in methanol and
5 acetonitrile had coefficient β values of 110%, 120% and 130%. In the case of methanol, 72.82
6 mg, 79.44 mg, 86.06 mg, of CBZ were respectively weighed out and taken in each of the
7 glass. In the case of acetonitrile, 38.72 mg, 42.24 mg, 45.76 mg were used. For each solution,
8 1ml was added to each tube. We used classical chromatography tubes that were adapted to fit
9 our experimental needs.³² The heating dissolution method was then used by placing the tubes
10 altogether in a bath (carrousel holder) for about 15 hours at 50 °C. After complete dissolution,
11 the solutions were cooled-down to 20 °C and then were aged from 1 to 2 days before
12 irradiation by LASER light at 20 °C. This ageing time permits the formation of clusters within
13 the solutions, thus increasing the probability of nucleation. The requirement for sample aging
14 was reinforced by subsequent work on glycine^{29-30,32} and L-histidine.³⁸

15
16 Moreover, proper experimental conditions were adopted in order to avoid photochemical
17 reaction resulting orange coloration (see section IV-2).
18
19

20 21 22 23 24 25 26 27 28 29 30 31 32 33 34 **III-5- CBZ crystals characterization**

35
36 The characterization of the obtained crystals forms was done both by Single crystal X ray
37 Diffraction ((Bruker[®] Diffraction D8 system at room temperature) and by morphology
38 observation under microscope (SEM).
39
40
41

42 43 44 45 46 47 48 49 50 51 52 53 54 55 56 57 58 59 60 **III-6- CBZ theoretical calculations**

61
62 In order to obtain a good and coherent estimate of the interaction energy for each pair of
63 molecules, a full *ab initio* computation was carried out using the same quantum chemistry
64 model within the functional density theory framework (M06-2X/cc-PVTZ), available from
65 the Gaussian09 software.⁶⁴

66
67 The choice for the M06-2X hybrid functional⁶⁵ was made in order to ensure a reliable
68 account for both short range and diffuse type interactions within and between rather remote
69 molecules. The correlation consistent triple zeta basis set⁶⁶ is known to be a good compromise
70

1
2
3 between cpu time to be devoted to each computation and the flexibility that is required for
4
5 giving a sufficient freedom for the electrons to reproduce the subtleties imposed by the
6
7 chemical bonds formations. For each crystalline form, the molecular geometries were taken
8
9 from experimental results. However, in many cases, because the published structures were
10
11 obtained by classical single crystal X-ray diffraction, the position of Hydrogen atoms had to
12
13 be determined from *ab initio* optimizations. Such an additional step is expected to be of
14
15 significant importance as many components of the interaction energies can safely be assumed
16
17 to rely on hydrogen interplay.
18
19

20
21 The computation of the interaction energy between two molecules A and B is of course
22
23 obtained from the subtraction $\Delta E = E_{A-B} - (E_A + E_B)$, where E_{A-B} is the energy for the pair
24
25 system, while E_A and E_B are the respective energies of isolated molecule A and molecule B.
26
27 All the geometries are here kept frozen as the purpose is to evaluate the interaction energy,
28
29 not the bonding energy. In that respect, it should be noted that some pairs were found to be
30
31 not bonded, i.e. the energy for the A-B system was higher than the sum of the energies for
32
33 each optimized subsystem.
34
35

36
37 However, if the interaction energy were to be estimated from the above mentioned
38
39 subtraction, a significant spurious bias would be introduced from the basis set superposition
40
41 error (BSSE) effect. This is well documented⁶⁷ and it is here sufficient to remind the reader
42
43 that, because the chosen (limited) basis set cannot account for all possible electrons behaviors,
44
45 electrons in system A-B are therefore offered more degree of freedom than in isolated
46
47 subsystems A or B. The reason is simply that each basis function is centered on a nucleus,
48
49 and, as such, for a given quantum chemistry model, the more atoms, the richer the basis set,
50
51 the larger it spans the configuration space. BSSE effects are thus very well known for
52
53 affecting in a large part the estimate in bonding energies and, in our case, interaction energies:
54
55 part of the difference in energies between A-B and (A,B) resulting from a mere change in the
56
57
58
59
60

1
2
3 basis set. In order to overcome that issue, one is thus led to compute each subsystem (isolated
4 molecules) using the basis set pertaining to the full system. The interaction energy is now
5 estimated using $\Delta E^{AB} = E^{AB}_{A-B} - (E^{AB}_A + E^{AB}_B)$, where the superscript now indicates that the
6 full A-B basis set is used for each subsystem. In the case of bonding computations, this
7 calculation is the first step of a method referred to as the “counterpoise correction”.

16 **IV Results and discussion**

18 **IV-1- CBZ metastable zone and spontaneous nucleation**

20 Figure 3b shows the solubility curves of CBZ (form III) in methanol and acetonitrile
21 reported in the literature⁶³ as well as metastable zone that we determined experimentally. As
22 reported in Figure 3b, the critical supersaturation β_c coefficient for the CBZ at 20 °C is about
23 130 % in methanol and about 140 % in acetonitrile leading to $\beta_{c,20, \text{methanol}} (72) = 130 \%$ and
24 $\beta_{c,20, \text{acetonitril}} (72) = 140 \%$, the absence of crystals were observed during an induction time of
25 72 hours. It should be noted that the metastable zone for acetonitrile is determined, following
26 the protocol described above for the case of methanol. The width of the metastable zone is
27 higher in acetonitrile than in methanol. Based on these experimental results, for a
28 supersaturation lower than $\beta_{c,20, \text{methanol}} (72)$ the solution could be considered as metastable.
29 Therefore, for NPLIN experiments, all the supersaturated solutions were prepared with a
30 supersaturation coefficient lower than 130 %. As a result, any crystallization from the solution
31 in these conditions under irradiation by an external field (LASER in this case) could be taken
32 as being due to LASER and therefore LASER can be considered as the cause of the induced
33 nucleation. It should be noted that, for each experiment, new HPLC tubes for our experiments
34 were used in order to avoid any heterogeneous or seeded nucleation.

35
36
37
38
39
40
41
42
43
44
45
46
47
48
49
50
51
52
53
54 After determining the metastable zone width, we have evaluated the impact of the solvent
55 on the spontaneous nucleation efficiency. To that end, different supersaturated solutions in
56
57
58
59
60

1
2
3 two solvents (methanol and acetonitrile) were prepared and stored in an environment at 20 °C
4
5 for the same period of time but sufficiently long to allow nucleation to begin (> 72 h). Figure
6
7 4 shows the fraction of tubes that have crystallized as a function of supersaturation
8
9 coefficient. The results clearly show that CBZ nucleation is more important in methanol than
10
11 in acetonitrile. This is in agreement with the higher solubility of CBZ in methanol (64 mg/ml)
12
13 as compared to that in acetonitrile (35.2 mg/ml) at 20 °C.⁶³ The influence of solubility on the
14
15 nucleation rate can be explained by the classical nucleation theory.⁶⁹ The classical nucleation
16
17 equation predicts that under constant supersaturation the rate of nucleation is faster in systems
18
19 with higher solubility. In both solvents the CBZ crystal is of form III as identified by its
20
21 morphology and habit. These results characterize the spontaneous nucleation of CBZ in
22
23 acetonitrile and methanol and will be used for the purpose of comparison with the case of
24
25 NPLIN.
26
27
28

29 **IV-2- Photochemical reaction inhibition**

30
31 During the experimental preliminary study, it was observed that CBZ solutions yield an
32
33 orange coloration upon exposition to the pulsed nanosecond LASER with wavelength of 532
34
35 nm, and an energy density in the range (0.3-0.45 GW/cm²). The hypothesis behind the orange
36
37 coloration is a photochemical reaction. Consequently, in order to showcase the impact of
38
39 LASER energy as well as the polarization on the nucleation efficiency, it is necessary to
40
41 exclude any possibility of nucleation due to photochemical reactions. This has been carried-
42
43 out by first characterizing the photo-chemical reaction. One notices a yellow-orange solution
44
45 coloration as shown in Figure 5. A spectroscopy-IR characterization allows to identify the
46
47 nature of the chemical compound responsible for the coloration. The obtained spectra are
48
49 provided in the supplementary materials part. According to the results of the characterization
50
51 of the CBZ in methanol solution and works reported in the literature^{8,70}, Iminostilbene (IMS)
52
53 is the compound responsible for the coloration (Figure 1b). The analysis of the chemical
54
55
56
57
58
59
60

1
2
3 formulas of both CBZ and IMS indicates similarities between the two chemical structures
4
5 except that, in the IMS molecule, CONH₂ is substituted by a Hydrogen atom. This can be
6
7 explained by the fact that the bond N-CONH₂ is broken due to LASER irradiation.
8
9 Furthermore, according to the works reported in the literature⁷¹, the binding energy of the N-
10
11 CONH₂ bond is the weakest in the CBZ molecule. The hypothesis made regarding the origin
12
13 of the hydrogen atom is either due to the presence of water molecules within the solvent or in
14
15 the ambient atmosphere through hydrolysis⁷² or from the solvent itself (methanol) through
16
17 photolysis.⁷³ To reduce the probability of generating IMS, strict anhydrous conditions were
18
19 respected when preparing the solutions mainly by working in an inert atmosphere and by a
20
21 pretreatment of the solvents with molecular sieves.⁷⁴ This is achieved by developing a specific
22
23 experimental bench composed of three main blocs: gloves box, argon gas bottle and vacuum
24
25 pump. The schematic diagram of the bench is detailed in the supplementary materials part.
26
27 The hypotheses regarding the origin of the transformation of CBZ to IMS, and thus the
28
29 presence of a Hydrogen in the solution, were validated by repeating the previous experiments
30
31 respecting strict anhydrous conditions as described and by observing the absence of solution
32
33 color change after laser irradiation. It has to be noticed that IMS is known as one of the most
34
35 important metabolite of CBZ.⁷⁵⁻⁷⁶

40 **IV-3- CBZ nucleation and crystallization from NPLIN**

41 *a) CBZ polymorphs and induction time reduction*

42
43
44 Crystal habit of CBZ, grown from pure methanol or acetonitrile under different conditions,
45
46 is observed under the microscope and are shown in Figure 6. In the case of acetonitrile, the
47
48 CBZ habits are either of needle-like or prism as shown in Figures 6a and 6b, respectively. The
49
50 obtained habits were also confirmed by using scanning electron microscopy (SEM) (Figure
51
52 7). According to the works reported in^{77,78}, a needle-like habit could be of polymorph I or II
53
54 while prism one is of polymorph III. For more precise identification, Single X-ray crystal
55
56 diffraction of both forms are compared to that reported in the Cambridge Structure Database
57
58
59
60

1
2
3 (CSD).^{8,69} Results are given in table 3 and confirm that needle-like habit corresponds to
4 polymorph I and prism habit to polymorph III.
5
6

7 For the sake of estimating the induction time after LASER solution irradiation, we depicted
8 in Figure 8, the evolution of solution nucleation as a function of the time. According to the
9 results given in Figure 8, 20 min were necessary for nucleation to occur (dark dots).
10 Simultaneously, a sample tube containing the same solution and prepared in the same
11 conditions but not exposed to LASER required more than 72 hours for the nucleation to
12 begin. Despite the ageing time (24 to 48 h) the exposed solutions remain in a metastable
13 state, while spontaneous nucleation occurs after 72h. These results clearly demonstrate that
14 the energy brought by LASER to the irradiated solution fosters nucleation and greatly reduces
15 the induction time. Moreover, it confirms that LASER beam power acts upon the primary
16 nucleation. It should be noticed that the nucleation occurs at the bottom of tubes.
17
18
19
20
21
22
23
24
25
26
27
28

29 ***b) Impact of irradiation energy and laser polarization on the nucleation efficiency***
30

31 The dependence of nucleation efficiency on LASER intensity is based on the preparation of
32 a large number of identical samples in strictly controlled conditions that would minimize the
33 variations between samples.^{60,78} We have exposed N samples to a given LASER intensity, and
34 we count the number of nucleated samples at this LASER intensity. If n samples nucleate, the
35 nucleation fraction is then given by n/N .
36
37
38
39
40
41

42 The nucleation efficiency depends on the supersaturation coefficient β as well as on the
43 laser irradiation energy density. Indeed, this is confirmed by the curves drawn in Figure 9 that
44 give the nucleation fraction as function of energy density for different supersaturation
45 coefficient values and LASER polarization. One can easily remark that, for both solvents and
46 polarization types (linear and circular), the higher β (within the metastable zone) and the
47 irradiation energy density, the higher the fraction of nucleated solution. Moreover, for both
48 solvents, the nucleation efficiency is slightly higher with CP LASER than LP LASER.
49
50
51
52
53
54
55
56
57
58
59
60

1
2
3 However, by comparing the solvent effect on CBZ nucleation, one can notice that the
4 nucleation (for $\beta = 110\%$) starts at a higher irradiation energy density level for acetonitrile.
5
6 This observation confirms the importance of solubility on nucleation: the higher the solubility
7
8 the easier the nucleation as pointed out previously.
9
10

11
12 ***c) Impact of laser polarization on CBZ polymorphs nucleated***
13

14 For three different values of β in acetonitrile and methanol and for linear and circular
15 LASER polarizations, we represented in Figure 10 the number of tubes that resulted in CBZ
16 polymorph of type I or III. The analysis of these graphs indicates that in acetonitrile, the
17 polymorph type is influenced by the LASER polarization. In the case of LP crystals nucleated
18 are mixtures of polymorphs I or III, but, in the case of CP, crystals nucleated are mainly the
19 polymorph III. In the case of the methanol, the resulting polymorph is of form III and it is
20 laser polarization independent. The identification has been done by Single Crystal X-ray
21 Diffraction for some crystals and extended to all sample by optical identification of the habit.
22
23
24
25
26
27
28
29
30

31 It should be noticed that CBZ molecule is the first organic drug molecule for which we
32 demonstrate that the LASER polarization has an impact on the crystal polymorphic form;
33
34 LASER polarization impact has been reported small organic molecules such as glycine and
35
36 histidine. According to Sun *et al*³² the polymorphism of glycine was absolutely controlled by
37
38 switching the LASER polarization in a specific range of supersaturation values (1.46–1.55),
39
40 leading to γ -polymorph and α -polymorph, for LP and CP respectively. Outside of this
41
42 supersaturation window, different polarizations yield the same polymorph. Yuyama *et al.*³⁴
43
44 demonstrated that under specific solution conditions: supersaturated or undersaturated or
45
46 saturated and under specific LASER polarization, it is possible to achieve a selective
47
48 fabrication of α and γ polymorphs of glycine. According to their results, for the
49
50 supersaturated/saturated solutions, the probability of γ -crystal preparation on the CP LASER
51
52 irradiation became higher at lower power compared to the LP one. Conversely, in the
53
54
55
56
57
58
59
60

1
2
3 unsaturated solution, the LP laser irradiation provided the higher preparation probability of γ -
4 form crystal compared to the CP one. Polarization switching has also been reported for L-
5 histidine.³⁸
6
7

9 **V- Some insight on the putative polarization switching nucleation mechanism**

10
11 One of the hypothesis of the NPLIN polarization switching is based on the pre-existence of
12 molecular clusters in the supersaturated solution. The provided explanation supposes that the
13 pre-existing clusters of rod-like type preferentially crystallize with a LP LASER beam while a
14 disk-like behavior will interact with a CP LASER beam.³² In order to estimate the symmetry
15 of the pre-existing clusters, we have to make the following assumptions: i) the symmetry of
16 the pre-clusters could be predicted through the symmetry of the final crystal packing; ii) the
17 nucleation is driven by the non-covalent bonds present in the final polymorphs; iii) the
18 relative intensity of these non-covalent bonds in the final polymorphs is considered as the
19 major criterion for predicting the symmetry of the pre-clusters.
20
21
22
23
24
25
26
27
28
29
30

31 We have identified in three CBZ polymorphs, I, II and III, the different pairs of molecules
32 formed by a CBZ molecule chosen as being a center molecule and each neighbor molecule is
33 linked by a non covalent bond (hydrogen bond or a short contact) to this center molecule. We
34 have excluded the CBZ IV according to the crystal habits observed after NPLIN nucleation
35 which differ from those observed by Lang *et al.*⁷⁹ Pairs of molecules, symmetry cards and
36 numbering are given in Figures S4, S5 and S6. For each pair, we have calculated the
37 theoretical interaction energy as defined in section III-6 (reported in Table S2). For CBZ III,
38 the interaction energy determined from an experimental charge density previously conducted
39 by El Hassan *et al.*⁷⁰ is also provided. Figure 11 represents the different arrangements as a
40 function of the interaction energy value. CBZ polymorph I presents four independent
41 molecules in the asymmetric unit. A careful examination of the equivalent pairs permits to
42 reduce the number of independent pairs from 28 to 16. Only the average value of the
43
44
45
46
47
48
49
50
51
52
53
54
55
56
57
58
59
60

1
2
3 interaction energy calculated over the four molecules of the asymmetric unit of CBZ I is
4
5 given in Figure 11. As the energy decreases, one can observe different behaviors. For an
6
7 energy interaction $< -64 \text{ kJ.mol}^{-1}$, the three polymorphs exhibit dimer clusters. At that energy
8
9 level one can consider that there is no difference between the three polymorphs. For an
10
11 interaction energy $< -39 \text{ kJ.mol}^{-1}$ CBZ III presents a 1-D symmetry (rod-like) which means
12
13 that, using the first two strongest interactions, the clusters formed in the supersaturated
14
15 solution would look as a chain. When considering an energy interaction $< -28 \text{ kJ.mol}^{-1}$, CBZ I
16
17 presents a 1-D symmetry using the first two strongest interactions, while CBZ II is of 1-D
18
19 symmetry using the first three strongest interactions. For an energy interaction $< -23 \text{ kJ.mol}^{-1}$,
20
21 CBZ III is of 3-D symmetry that takes into account the first four interactions.
22
23

24
25 It appears therefore that at an energy $< -23 \text{ kJ.mol}^{-1}$ CBZ I and CBZ II exhibit a more rod-
26
27 like behavior than CBZ III. These results seem to be in agreement with the polarization
28
29 switching observed with the acetonitrile solvent. The aforementioned analysis relies on the
30
31 assumption that the nucleation is driven by the non-covalent interactions existing in the final
32
33 crystal. This assumption makes use of the reported work on the nucleation theory based on the
34
35 bond orientational order.⁸⁰
36
37

38
39 As reported in Figure 10, the CBZ nucleation through NPLIN technique in methanol
40
41 solvent gives only the polymorphic form III. We have examined the non-covalent interactions
42
43 which exist between a CBZ molecule and a fragment $\text{C}\equiv\text{N}$ and OH *via* the use of the CSD.⁸¹
44
45 Among 59 structures including true polymorphs, hydrate, solvate and cocrystals (70 hints)
46
47 None of them shows a non-covalent interaction such as $(\text{NH}\dots\text{N}, \text{CH}\dots\text{N})$ with nitrile moiety,
48
49 while $\text{CH}\dots\text{O}$, $\text{NH}\dots\text{O}$ and $\text{OH}\dots\text{O}$ are present in a dozen of structures (figure S6). Therefore
50
51 in the CBZ supersaturated solution in methanol, the solvent could easily make short contacts
52
53 enabling the formation of form I or II. Methanol solvent could be seen as a crystallization
54
55
56
57
58
59
60

1
2
3 inhibitor of CBZ I. As shown in Figure 11, form III could easily crystallize through its π - π
4
5 interaction.

6
7 Moreover, the fact that one have crystallized form III and form I is coherent with the
8
9 relative stability of the first two most stable forms of CBZ.
10

11 12 13 **VI- Conclusion**

14
15 The work presented in this paper demonstrates for the first time the application of NPLIN on
16
17 drugs. The experimental work focused on the nucleation of CBZ molecules in methanol and
18
19 in acetonitrile. The metastable zone of the CBZ was determined at different temperatures in
20
21 both solvents and different supersaturated solutions were used. The nucleation evolution of
22
23 both solutions after irradiation by LASER beam of different energy density levels was
24
25 monitored by depicting photographs of the observed tube at regular time intervals. Irradiating
26
27 the solutions by LASER permitted to launch nucleation in the metastable zone and to reduce
28
29 the induction time from 72 h to about 20 min. The nucleation efficiency depends both on the
30
31 supersaturation coefficient as well as on the LASER energy density. It was indeed found that
32
33 the nucleation efficiency increases with the energy density carried by the LASER beam.
34
35 Moreover, the CP LASER beam polarization leads to a slightly higher nucleation efficiency
36
37 than the LP polarization. The LASER polarization affects the type of resulting polymorph.
38
39 The irradiation of acetonitrile by CP laser results in form III crystal while LP laser produces
40
41 form I and form III. The theoretical interaction energy were calculated and permitted to check
42
43 that the CBZ I is of rod-like type. This is in agreement with the reported explanation
44
45 supposing that the pre-existing clusters of rod-like type preferentially crystallize with a LP
46
47 LASER beam while a disk-like behavior interact with a CP LASER beam.³²
48
49
50
51
52
53
54

55 **Supplementary Material**

56
57
58
59
60

1
2
3 Details of the lattice data for the four anhydrous polymorphic forms of CBZ extracted from
4 the Cambridge Database (CSD). Theoretical and experimental interaction energy (KJ.mol⁻¹)
5 data for CBZ polymorph III, I and II. Symmetry card and non covalent interaction label for
6 CBZ polymorph I, II and III. FT-IR spectra of anhydrous CBZ polymorph III and
7 Iminostilbene. A schematic diagram representation of the experimental bench. Pairs of
8 molecules used in the calculation of CBZ I, CBZ II, and CBZ III. Results on the non-covalent
9 interaction in the structures reported in the CSD and that contain a CBZ molecule. This
10 material is available free of charge via the Internet at <http://pubs.acs.org>.
11
12
13
14
15
16
17
18
19

20 21 **Acknowledgements** 22

23 The authors would thank Pr Nour Eddine Ghermani (Institut Gallien, University Paris-Sud)
24 for Single Crystal Diffraction measurements and constructive discussion. This project has
25 been funded through an ANR P2N project NPLIN_4_drug.
26
27
28
29
30
31
32
33
34
35
36
37
38
39
40
41
42
43
44
45
46
47
48
49
50
51
52
53
54
55
56
57
58
59
60

Bibliographic references

- 1
2
3
4
5 [1] Shekunov, B.Y.; York, P. *J. Cryst. Growth.* **2000**, *211*, 122–136.
6
7
8 [2] Mangin, D.; Puel, F.; Veessler, S. *Org. Process Res. Dev.* **2009**, *13*, 1241-1253
9
10
11 [3] Rodriguez-Spong B., Price C., Jayasankar A., Matzger A.,J., Rodriguez-hornedo N. *Adv*
12
13 *Drug Deliver Rev.* **2004**, *56*, 241-274
14
15
16 [4] Huang, L.F.; Tong, W. *Adv Drug Deliver Rev.* **2004**, *56*, 241-274.
17
18
19 [5] Price, S.L. *Adv Drug Deliver Rev.* **2004**, *56*, 301-319.
20
21
22 [6] Chemburkar, S.R.; Baue, r J.; Deming, K.; Spiwek, H.; Patel, K.; Morris, J.; Henry, R.;
23
24 Spanton, S.; Dziki, W.; Porter, W.; Quick, J.; Bauer P.; Donaubaue, J.; Narayanan, B.A.;
25
26 Soldani, M.; Riley, D.; McFarland, K. *Org. Proc. Res. Dev.* **2000**, *4*, 413–417.
27
28
29 [7] Garetz, B., A., Aber, J., E., Goddard, N., L., Young, R., G., Myerson, A., S. *Phys. Rev.*
30
31 *Lett.* **1996**, *77*, 3475 - 3476
32
33
34 [8] Grzesiak, A.L.; Lang, M.; Kim, K.; Matzger, A.J. *J. Pharm. Sci.* **2003**, *92*, 2261-2271.
35
36
37 [9] Florence, A.J.; Johnston, A.; Price, S.L.; Nowell, H.; Kennedy, A.R.; Shankland, N. *J.*
38
39 *Pharm. Sci.* **2006**, *95*, 1918-1930.
40
41
42 [10] Lohani, S.; Zhang, Y. G.; Chyall, L. J.; Mougin-Andres, P. F.; Muller, X.; Grant, D. J.
43
44 *W.Acta Crystallogr. Sect. E.* **2005**, *61*, 1310-1312.
45
46
47 [11] Detoisien, T.; Forite, M.; Taulelle, P.; Teston,J.; Colson, D.; Klein,J.P.; Veessler, S. *Org.*
48
49 *Process Res. Dev.* **2009**, *13*, 1338–1342.
50
51
52 [12] Virone, C.; Kramer, H. J. M.; Van Rosmalen, G. M.; Stoop, A. H.; Bakker, T. W. *J.*
53
54 *Cryst. Growth* **2006**, *294*, 9.
55
56
57
58
59
60

1
2
3 [13] Ruecroft, G.; Hipkiss, D.; Ly, T.; Maxted, N.; Cains, P. W. *Org. Process Res. Dev.*
4
5 **2005**, *9*, 923.

6
7
8 [14] Lyczko, N.; Espitalier, F.; Louisnard, O.; Schwartzentruber, J. *Chem. Eng. J.* **2002**, *86*,
9
10 233.

11
12
13 [15] Taleb, M.; Didierjean, C.; Jelsch, C.; Mangeot, J. P.; Capelle, B.; Aubry, A. *J. Cryst.*
14
15 *Growth* **1999**, *200*, 575.

16
17
18 [16] Moreno, A.; Sazaki, G. *J. Cryst. Growth*, **2004**, *264*, 438.

19
20
21 [17] Penkova, A.; Gliko, O.; Dimitrov, I. L.; Hodjaoglu, F. V.; Nanev, C.; Vekilov, P. G. *J.*
22
23 *Cryst. Growth*, **2005**, *275*, e1527.

24
25
26 [18] Hammadi, Z.; Veesler, S. *Prog Biophys Mol Biol* **2009**, *101*, 38-44.

27
28
29 [19] Revalor, E.; Hammadi, Z.; Astier, J.P.; Grossier, R.; Garcia, E, Hoff, C.; Furuta, K.;
30
31 Okustu, T.; Morin, R.; Veesler S. *J. Cryst. Growth*, **2010**, *310*, 939-946.

32
33
34 [20] Voss, D. *Science* **1996**, *274*, 1325.

35
36
37 [21] Oxtoby, D.W. *Nature* **2002**, *420*, 277–278.

38
39
40 [22] Okutsu, T.; Nakamura, K.; Haneda, H.; Hiratsuka, H. *Cryst. Growth Des.* **2004**, *4*, 113-
41
42 115.

43
44
45 [23] Tyndall, J. *Philos. Mag.* **1896**, *37*, 384.

46
47
48 [24] Okutsu, T.; Furuta, K.; Terao, T.; Hiratsuka, H.; Yamano, A.; Ferté, N.; Veesler, S.
49
50 *Cryst. Growth Des.* **2005**, *5*, 1393–1398.

51
52
53 [25] Veesler, S.; Furuta, K.; Horiuchi, H.; Hiratsuka, H.; Ferté, N.; Okutsu, T. *Cryst. Growth*
54
55 *Des.* **2006**, *6*, 1631–1635.

- 1
2
3 [26] Okutsu, T.; Furuta, K. K.; Watanebe, I.; Mori, H.; Obi, K.; Horota, K.; Horiuchi, H.;
4
5 Sazaki, G.; Veessler, S.; Hiratsuka, H.J. *Photochem. Photobiol. A Chem.* **2007**, *190*, 88–93.
6
7
8 [27] Furuta, K.; Horiuchi, H.; Hiratsuka, H.; Okutsu, T. *Cryst. Growth Des.* **2008**, *8*, 1886-
9
10 1889.
11
12
13 [28] Tam, A.; Moe, G.; Happer, W. *Phys. Rev. Lett.* **1975**, *35*, 1630–1633.
14
15
16 [29] Zaccaro, J.; Matic, J.; Myerson, A.S.; Garetz, B.,A. *Cryst. Growth Des.* **2001**, *1*, 5-8.
17
18
19 [30] Garetz, B. A.; Matic, J. *Phys. Rev. Lett.* **2002**, *89*, 175501.
20
21
22 [31] Clair, B.; Ikni, A.; Scouflaire, P.; Quemener, V.; Spasojević-de Biré, A. submitted to J.
23
24 App. Cryst. **2014**
25
26
27 [32] Sun, X.; Garetz, B.; A. *Cryst. Growth Des.* **2006**, *6*, 684-689.
28
29
30 [33] Rungsimanon, T.; Yuyama, K.; Sugiyama, T.; Masuhara, H. *Cryst. Growth Des.* **2010**,
31
32 *10*, 4686-4688.
33
34
35 [34] Yuyama, K.; Rungsimamon, T.; Sugiyama, T.; Masuhara, H. *Cryst. Growth Des.* **2012**,
36
37 *12*, 2427 - 2434.
38
39
40 [35] Uwada, T.; Fuji, S.; Sugiyama, T.; Usman, A.; Miura, A.; Masuhara, H.; Kanaizuka,
41
42 K.; Haga, M. *Appl Mater Interfaces*, **2012**, *4*, 1158-1163.
43
44
45 [36] Liu, T. H.; Uwada, T.; Sugiyama, T.; Usman, A.; Hosokawa, Y.; Masuhara, H.;
46
47 Chiang, T. W.; Chen, C. J. *J. Cryst. Growth*, **2013**, *366*, 101-106.
48
49
50 [37] Matic, J.; Sun, X.; Garetz, B. A. *Cryst. Growth Des.* **2005**, *5*, 1565-1567.
51
52
53 [38] Sun, X.; Garetz, B., A.; Myerson, A. S. *Cryst. Growth Des.* **2008**, *8*, 1720-1722.
54
55
56
57
58
59
60

1
2
3 [39] Tsunesada, F.; Iwai, T.; Watanabe, T.; Adachi, H.; Yoshimura, M.; Mori, Y.; Sasaki, T.
4
5 *J. Cryst. Growth* **2002**, *237*, 237-239.

6
7
8 [40] Hosokawa, Y.; Adachi, H.; Yoshimura, M.; Mori, Y.; Sasaki, T.; Masuhara, H. *Cryst.*
9
10 *Growth Des.* **2005**, *5*, 861-863.

11
12
13 [41] Ward, M.R.; McHugh, S.; Alexander, A. J. *Phys. Chem.* **2012**, *14*, 90-93.

14
15
16 [42] Alexander, A. J.; Camp, P. J. *Cryst. Growth Des.* **2009**, *9*, 958-963.

17
18
19 [43] Duffus, C.; Camp, P. J.; Alexander, A. J. *J. Am. Chem. Soc.* **2009**, *131*, 11676-11677.

20
21
22 [44] Ward, M. R.; Ballingall, I.; Costen, M.L.; McKendrick, K.G.; Alexander, A.J. *Chem.*
23
24 *Phys. Lett.* **2009**, *481*, 25-28.

25
26
27 [45] Ward, M.R.; Alexander, A. J. *Cryst. Growth Des.* **2012**, *12*, 4554-4561.

28
29
30 [46] Ward, M. R.; Copeland, G. W.; Alexander, A. J. *J. Chem. Phys.* **2011**, *135*, 114508-
31
32 114516.

33
34
35 [47] Soare, A.; Dijkink, R.; Pascual, M. R.; Sun, C.; Cains, P. W.; Lohse, D.; Stankiewicz,
36
37 A. I.; Kramer, H. J. M.; *Cryst. Growth Des.* **2011**, *11*, 2311-2316.

38
39
40 [48] Jacob, J.A.; Sorgues, S.; Dazzi, A.; Mostafavi, M.; Belloni, J. *Cryst. Growth Des.*
41
42 **2012**, *12*, 5980-5985.

43
44
45 [49] Adachi, H.; Takano, K.; Hosokawa, Y.; Inoue, T.; Mori, Y.; Matsumura, H.;
46
47 Yoshimura, M.; Tsunaka, Y.; Morikawa, M.; Kanaya, S.; Masuhara, H.; Kai, Y.; Sasaki, T.
48
49 *Jpn. J. Appl. Phys.* **2003**, *42*, L798-L800.

50
51
52 [50] Lee, I.S.; Evans J.M.B.; Erdemir, D.; Lee, A. Y.; Garetz, B.A.; Myerson, A.S. *Cryst.*
53
54 *Growth Des.* **2008**, *8*, 4255-4261

- 1
2
3 [51] Tsuboi, Y.; Shoji, T.; Kitamura, N. *Jpn. J. Appl. Phys.* **2007**, *46*, L1234.
4
5
6 [52] Sugiyama, T.; Adachi, ; Masuhara, H. *Chem. Lett.* **2007**,*36*,1480-1481.
7
8
9 [53] Nakamura, K.; Sora, Y.; Yoshikawa, H.Y.; Hosokawa, Y.; Murai, R.; Adachi, H.;
10 Mori, Y.; Sasaki, T.; Masuhara, H. *Appl. Surf. Sci.* **2007**, *253*, 6425-6429.
11
12
13
14 [54] Yoshikawa, H.Y.; Murai, R.; Sugiyama, S.; Sazaki, G.; Kitatani, T.; Takahashi, Y.;
15 Adachi, H.; Matsumura, H.; Murakami, S.; Inoue, T.; Takano, K.; Mori, Y. *J. Cryst. Growth*,
16
17 **2009**, *311*, 956-959.
18
19
20
21 [55] Hammadi Z.; Astier J. P.; Morin R.; Veessler S. *Cryst. Growth Des.* **2009**, *9*, 3346-
22 3347.
23
24
25
26 [56] Murai, R.; Yoshikawa, H. Y.; Takahashi, Y.; Maruyama, M.; Sugiyama, S.; Sazaki, G.;
27 Adachi, H.; Takano, K.; Matsumura, H.; Murakami, S.; Inoue, T.; Mori, Y. *Appl. Phys. Lett.*,
28
29 **2010**, *96*, 043702.
30
31
32
33
34 [57] Yennawar, N.; Denev, S.; Gopalan, V.; Yennawar, H. *Acta Cryst.* **2010**, *F66*, 969-972.
35
36
37 [58] Murai, R.; Yoshikawa, H.Y.; Hasenka, H.; Takahashi, Y.; Maruyama, M.; Sugiyama,
38 S.; Adachi, H.; Takano, K.; Matsumura, H.; Murakami, S.; Inoue, T.; Mori, Y. *Chem. Phys.*
39 *Lett.* **2011**, *510*, 139-142.
40
41
42
43 [59] Nakayama, S.; Yoshikawa, H.Y.; Murai, R.; Kurata, M.; Maruyama, M.; Sugiyama, S.;
44 Aoki, Y.; Takahashi, Y.; Yoshimura, M.; Nakabayashi, S.; Adachi, H.; Matsumura, H.; Inoue,
45 T.; Takano, K.; Murakami, S.; Mori, Y. *Cryst. Growth Des.* **2013**, *13*, 1491-1496.
46
47
48
49
50 [60] Sun, X.; Garetz, B. A. *Phys. Rev. E*, **2009**, *79*, 021701.
51
52
53
54
55 [61] Knott, B.C.; LaRue, J.L.; Wodtke, A.M.; Doherty, M.F.; Peters, B. *J. Chem. Phys.*
56 **2011**, *134*, 171102
57
58
59
60

1
2
3 [62] Kashchiev, D.; Verdoes, D; Vanrosmalen, GM *J. Cryst. Growth*, **1991**, *110*, 373-380.

4
5
6 [63] O'Mahony, M. A.; Maher, A.; Croker, D. M.; Rasmuson, Å. C.; Hodnett, B. K. *Cryst.*
7
8 *Growth Des.* **2012**, *12*, 1925-1932.

9
10
11 [64] Gaussian 09, Revision D.01, Frisch, M.J.; Trucks, G. W.; Schlegel, H. B.; G. E.;
12
13 Scuseria, Robb, M. A.; Cheeseman, J. R.; Scalmani, G.; Barone, V.; Mennucci, B.; Petersson,
14
15 G. A.; Nakatsuji, H.; Caricato, M.; Li, X.; Hratchian, H. P.; Izmaylov, A. F.; Bloino, J.;
16
17 Zheng, G.; Sonnenberg, J. L.; Hada, M.; Ehara, M.; Toyota, K.; Fukuda, R.; Hasegawa, J.;
18
19 Ishida, M.; Nakajima, T.; Honda, Y.; Kitao, O. ; Nakai, H.; Vreven, T.; Montgomery, J. A.;
20
21 Peralta, Jr. J. E.; Ogliaro, F.; Bearpark, M.; Heyd, J. J.; Brothers, E.; Kudin, K. N.;
22
23 Staroverov, V. N.; Kobayashi, R.; Normand, J.; Raghavachari, K.; Rendell, A.; Burant, J. C.;
24
25 Iyengar, S. S.; Tomasi, J.; Cossi, M.; Rega, N.; Millam, J. M.; Klene, M.; Knox, J. E.; J. B.;
26
27 Cross, Bakken, V.; Adamo, C.; Jaramillo, J.; Gomperts, R.; Stratmann, R. E.; Yazyev, O.;
28
29 Austin, A. J.; Cammi, R.; Pomelli, C.; Ochterski, J. W.; Martin, R. L.; Morokuma, K.;
30
31 Zakrzewski, V. G.; Voth, G. A.; Salvador, P.; Dannenberg, J. J.; Dapprich, S.; Daniels, A. D.;
32
33 Farkas, Ö.; Foresman, J. B.; Ortiz, J. V.; Cioslowski, J.; Fox, D. J. *Gaussian, Inc.,*
34
35 *Wallingford CT, 2009.*

36
37
38
39
40
41 [65] Zhao, Y.; Truhlar, D.G. *Theor Chem. Acc.* **2008**, *120*, 215-241

42
43
44 [66] Dunning, T. H. Jr., *J. Chem. Phys.* **1989**, *90*, 1007-23.

45
46
47 [67] Boys, S. F.; Bernardi, F. *Mol. Phys.* **1970**, *19*, 553-566.

48
49
50 [68] Mullin, J. W. *Crystallization*. 4th ed.; Butterworth-Heinemann; Oxford, 2001.

51
52
53 [69] Kuramshina, G.M.; Mogi, T.; Takahashi, H. *J. Mol. Struct.* **2003**, *661-662*, 121-139.

54
55
56 [70] McNaught, A. D.; Wilkinson, A. Blackwell Scientific Publications, Oxford, **1997**.

1
2
3 [71] El Hassan, N.; Ikni, A.; Gillet, J.M.; Spasojevic-de Biré, A.; Ghermani, N.E. *Cryst.*
4
5 *Growth Des.* 2013, *13*, 2887-2896.

6
7
8 [72] Buenker, R.J.; Olbrich, G.; Schuchmann, H.P.; Schurmann, B.I.; von Sonntag, C. *J.*
9
10 *Am. Chem. Soc.* **1984**, *106*, 4362-4368.

11
12
13 [73] Bradley, D.; Williams, G.; Lawton, M. *J. Org. Chem.* **2010**, *75*, 8351–8354.

14
15
16 [74] Mathieu, O; Picot, MC; Gelisse, P; Breton, H; Demoly, P; Hillaire-Buys, D.
17
18 *Pharmacol. Rep.* **2011**, *63*, 86-94.

19
20
21 [75] Dzodic, PL; Zivanovic, LJ; Protic, AD; Zecevic, ML; Jovic, BM *J. AOAC Int.* **2010**,
22
23 *93*, 1059-1068.

24
25
26 [76] Rustichelli, C.; Gamberini, G.; Ferioli, V.; Gamberini, M.C.; Ficarra, R.; Tommasini
27
28 *S. J. Pharm. Biomed. Anal.* **2000**, *23*, 41-54.

29
30
31 [77] Ceolin, R.; Toscani, S.; Gardette, M.F.; Agafonov, V.; Dzyabchenko, A.; Bacheti, B. *J.*
32
33 *Pharma. Sci.*, **1997**, *86*, 1062-1065.

34
35
36 [78] Spasojević - de Biré, A. *International Innovation*, **2013**, 45-49.

37
38
39 [79] Lang, M.; KampF, J.W.; Matzger, A. *J. J. Pharma.Sci.*, 2002, *91*, 1186-1190.

40
41
42 [80] Russo, J.; Tanaka, H. *AIP Conference Proceedings*, **2013**, *1518*, 232-237.

43
44
45 [81] Allen, F. H. *Acta Crystallogr.*, **2002**, *B58*, 380-388,
46
47
48
49
50
51
52
53
54
55
56
57
58
59
60

1
2
3 **Table captions**
4
5
6

7 **Table 1.** NPLIN on different compounds as reported in the literature. Laser type P = Pulsed
8 LASER, CW = Continuous Wave LASER. Pulsation length : fs = femto-second, ps = pico-
9 second, ns = nano-second, foc = focalized, nfoc = not focalized, LP = Linear Polarization, CP
10 = Circular Polarization
11
12
13
14
15

16 **Table 2.** Experimental conditions for metastable zone width determination.
17
18

19 **Table 3.** Characterization of crystal obtained by laser irradiation of CBZ solutions by Single
20 crystal X-ray diffraction.
21
22
23
24
25
26
27
28
29
30
31
32
33
34
35
36
37
38
39
40
41
42
43
44
45
46
47
48
49
50
51
52
53
54
55
56
57
58
59
60

1
2
3 **Figures captions**
4
5
6

7 **Figure 1.** Molecular structure of Carbamazepine (a) and Iminostilbene (b)
8
9

10 **Figure 2.** Schematic representation of motorized LASER irradiation set-up
11
12

13 **Figure 3.** (a) Schematic illustration of the method used to determine the metastable zone of
14 CBZ with in situ microscopy: CBZ solubility (blue curve); metastable limit zone (black
15 curve); heat to complete dissolution (red arrow); cool to supersaturation (green arrow).
16 Circles illustrate different solution concentrations tested at the chosen temperature: empty
17 circles (not crystallized), filled circles (crystallized). (b) Metastable zone limit of
18 carbamazepine in methanol (bleu symbols) and in acetonitrile (green symbols). Red symbols
19 and black correspond respectively to solubility curves of CBZ in acetonitrile and methanol
20 according to.⁶³
21
22
23
24
25
26
27
28
29
30

31 **Figure 4.** Fraction of CBZ solution nucleated after $t > 72$ h as function of supersaturation
32 coefficient in absence of LASER irradiation, red symbols correspond to acetonitrile and black
33 symbols correspond to methanol at 20 °C.
34
35
36
37
38

39 **Figure 5.** CBZ in methanol solution color change after LASER irradiation (a) before
40 irradiation (b) after irradiation.
41
42
43

44 **Figure 6.** Micrographs of crystal obtained by LASER irradiation of CBZ solutions, (a), (b) in
45 acetonitrile and (c) in methanol, scale bar 100 μm
46
47
48

49 **Figure 7:** SEM micrographs of CBZ crystals produced by NPLIN in acetonitrile, (a) form III
50 and (b) form I
51
52
53
54
55
56
57
58
59
60

1
2
3 **Figure 8:** *In situ* monitoring of nucleation progress after irradiation: CBZ in acetonitrile,
4 supersaturation coefficient 130 %, LASER energy density 0.3 GW/cm², LP, irradiation time 1
5 min, scale bar 100 μm
6
7
8

9
10 **Figure 9.** Impact of LASER energy and polarization on CBZ nucleation in both methanol and
11 acetonitrile
12
13

14
15 **Figure 10.** Impact of supersaturation coefficient and LASER polarization on the CBZ
16 nucleation and crystal forms.
17
18

19
20 **Figure 11.** Interaction energy (KJ.mol⁻¹) for CBZ polymorphic form I, II and III versus the
21 rank of the interaction energy (1 is the strongest interaction for each polymorph). The
22 interaction type is indicated in blue in each range of interaction energy. The packing
23 corresponding to the different range of interaction is given for each polymorph in decreasing
24 order of stability. Symmetry of these packing is indicated in red. The green triangle
25 corresponds to the average values over the four independent molecule of the asymmetric unit.
26
27 For the form III with the interaction energy < -23 KJ.mole⁻¹ the projection along a, b and c
28 axis is given in order to better demonstrate the 3-D character of the packing.
29
30
31
32
33
34
35
36
37
38
39
40
41
42
43
44
45
46
47
48
49
50
51
52
53
54
55
56
57
58
59
60

Table 1

Compound		Solvent	Year	Ref.	LASER type	λ (nm)	Polymorph control through laser polarization
Organic	Urea	Water	1996	7	P, ns nfoc	1064	
			2005	37	P, ns,nfoc	1064	
	Glycine	Water	2001	28	P, ns nfoc	1064	
			2002	29	P, ns,nfoc	1064	
			2006	32	P, ns,nfoc	1064	
			2010	33	CW, foc	1064	
		Heavy Water	2012	34	CW, foc	1064	<i>Saturated/Supersaturated solutions</i> - CP laser irradiation enhances γ -polymorph , - LP irradiation enhances α -polymorph. <i>Unsaturated solutions:</i> - LP irradiation enhances γ -Polymorph, - CP irradiation enhances α - polymorph.
	Water	2012	35	CW, foc	1064		
		2013	36	P, fs, foc	780		
	L-Histidine	Water	2008	38	P, ns,nfoc	532	<i>Supersaturated solutions</i> - Circularly polarized light favors the formation of polymorph A, - Linearly polarized light favors the formation of a mixture of polymorphs A and B.
	DAST	Water	2002	39	P, ns, foc	1064	
		Methanol	2005	40	P, fs, foc	800	
	Glacial acetic acid	-	2012	41	P, ns, nfoc	1064	
Inorganic	KCl	Water	2009	42	P, ns,nfoc	1064	
		agarose gel / water	2009	43	P, ns,nfoc	1064	

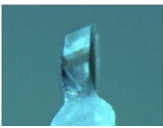
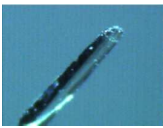
		Water	2009	44	P, ns,nfoc	1064
	KCl & KBr	Water	2012	45	P, ns, nfoc	532 1064
	NaClO ₃	-	2011	46	P, ns, foc	1064
	(NH ₄) ₂ SO ₄ & KMnO ₄	methanol / ethanol	2011	47	P, ns, foc	532
	KNO ₃	Water	2012	48	P, ns, foc	532
Protein	Lysozyme	Sodium acetate buffer	2003	49	P, fs, foc	780
	Lysozyme /BPT	Sodium acetate buffer	2008	50	P, ns,nfoc	1064
	Lysozyme	Heavy Water/ Sodium acetate buffer/NaCl	2007	52	CW, foc	1064
		Sodium acetate buffer / Gel medium (PEG 6000)	2007	53	P, fs, foc	780
	Lysozyme, Thaumatin	agarose gel / N-[2-acetamido]-2-iminodiacetic acid (ADA)	2009	54	P, fs, foc	780
	Lysozyme	agarose gel / NaAc buffer	2010	56	P, fs, foc	780
	Lysozyme, Ribonuclease B, sorbitol dehydrogenase, Glucose dehydrogenase, Fructose dehydrogenase, myoglobin,	-	2010	57	P, ps, foc	532
	Lysozyme	Sodium acetate buffer	2011	58	P, fs, foc	780
		agarose gel / Sodium acetate buffer/NaCl	2013	59	P, fs, foc	780/ 800
Miscellaneous	Supercooled 4- <i>n</i> -pentyl-4-cyanobiphenyl (5CB) liquid crystal	-	2012	60	P, ns, nfoc	1064

	Alkali-Metal vapor	-	1975	26	CW, foc	589	
	Carbonated water		2011	61			

Table 2

Supersaturation coefficient ($\beta\%$)	Carbamazepine concentration (mg. CBZ/ml. Acetonitrile)				Carbamazepine concentration (mg. CBZ/ml. MeOH)			
	at 5°C	at 20°C	at 30°C	at 40°C	at 5°C	at 20°C	at 30°C	at 40°C
110	24,6	38,7	52,8	71,2	47,8	72,8	98,2	132,8
120	26,8	42,2	57,6	77,7	52,2	79,4	107,1	144,9
130	29,1	45,7	62,4	84,2	56,5	86,1	116,1	157,0
140	31,3	49,2	67,2	90,7	60,9	92,6	125,0	169,1
150	33,6	52,8	72,0	97,2	65,2	99,3	133,9	181,2

Table 3

Crystal tested by D8		Recode from CSD CBMZPN01		Recode from CSD CBMZPN11
Space group	P2 ₁ /n	P2 ₁ /n	P-1	P-1
a (Å), α(°)	7.533(4), 90	7.537(1), 90	5.275(5), 84.19(3)	5.1705(6), 84.124(4)
b (Å), β(°)	11.154(6), 92.81(2)	11.156(2), 92.86(2)	20.720(14), 87.88(3)	20.574(2), 88.008(4)
c (Å), γ(°)	13.896(7), 90	13.912(3), 90	22.383(17), 85.37(4)	22.245(2), 85.187(4)
Lattice system	P-Monoclinic	P-Monoclinic	Triclinic	Triclinic
Crystal Habit	Prisms	Prisms	Needle	Needle

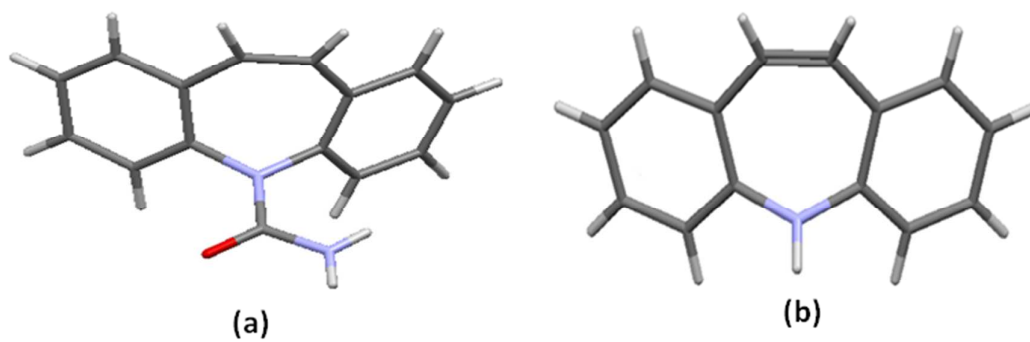


Figure 1

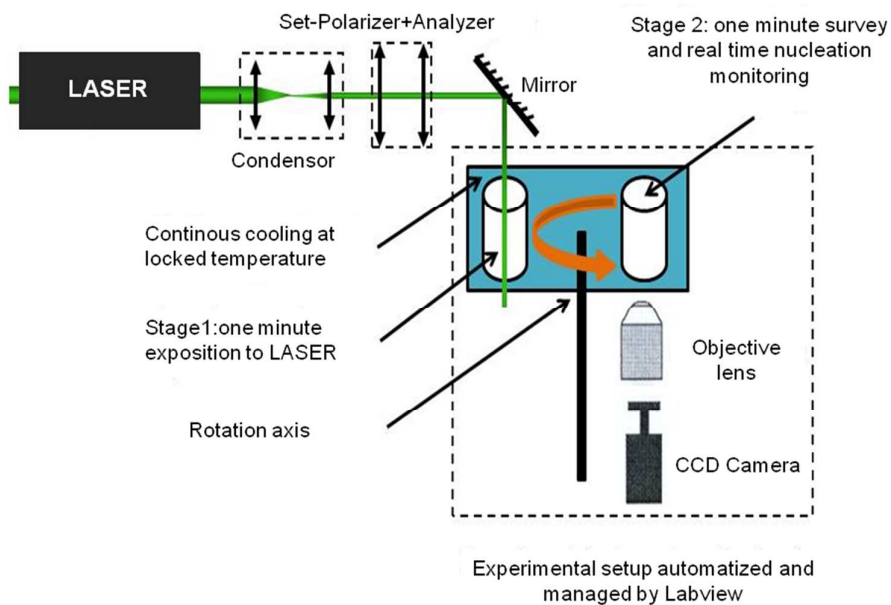


Figure 2

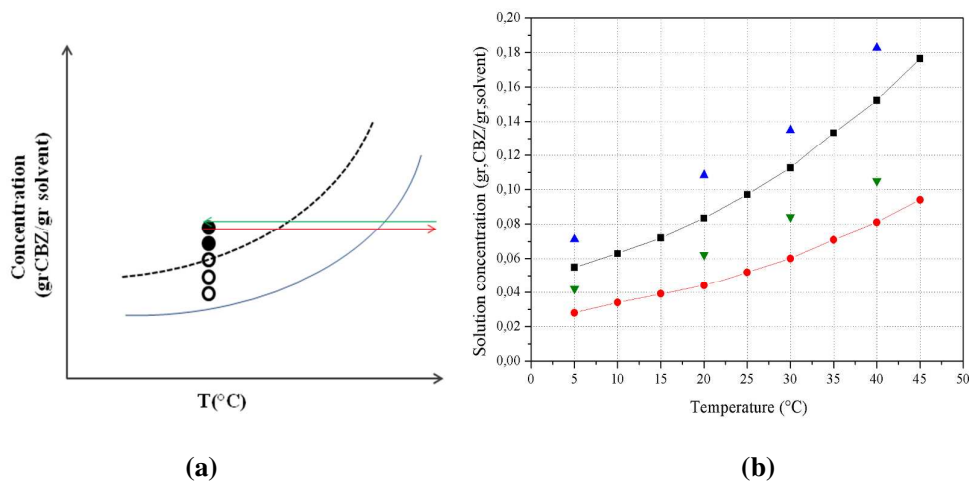


Figure 3

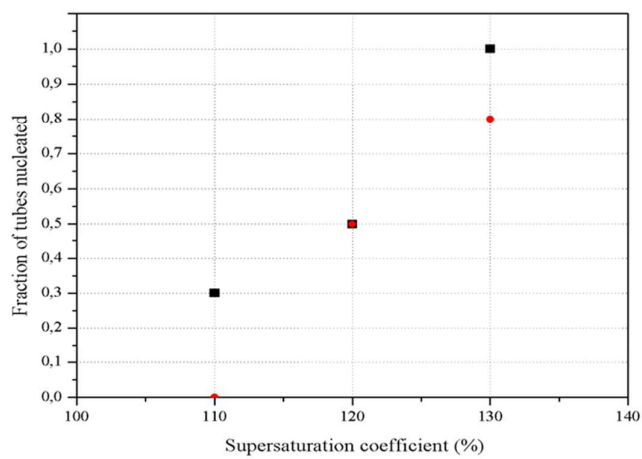
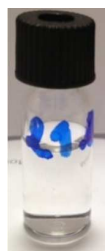
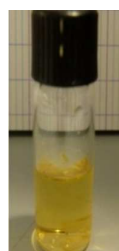


Figure 4

1
2
3
4
5
6
7
8
9
10
11
12
13
14
15
16
17
18
19
20
21
22
23
24
25
26
27
28
29
30
31
32
33
34
35
36
37
38
39
40
41
42
43
44
45
46
47
48
49
50
51
52
53
54
55
56
57
58
59
60



(a) Before chemical reaction



(b) After photo-chemical reaction

Figure 5

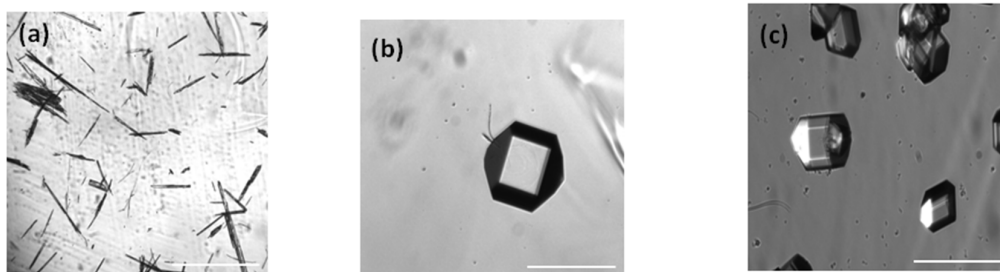


Figure 6

1
2
3
4
5
6
7
8
9
10
11
12
13
14
15
16
17
18
19
20
21
22
23
24
25
26
27
28
29
30
31
32
33
34
35
36
37
38
39
40
41
42
43
44
45
46
47
48
49
50
51
52
53
54
55
56
57
58
59
60

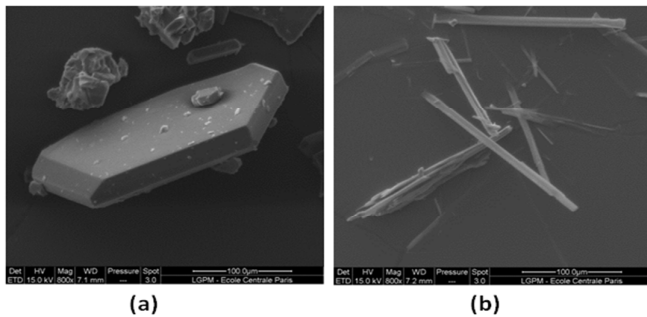


Figure 7

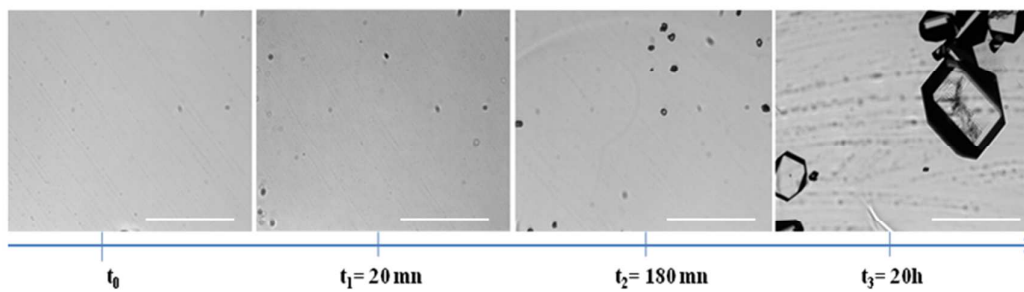


Figure 8

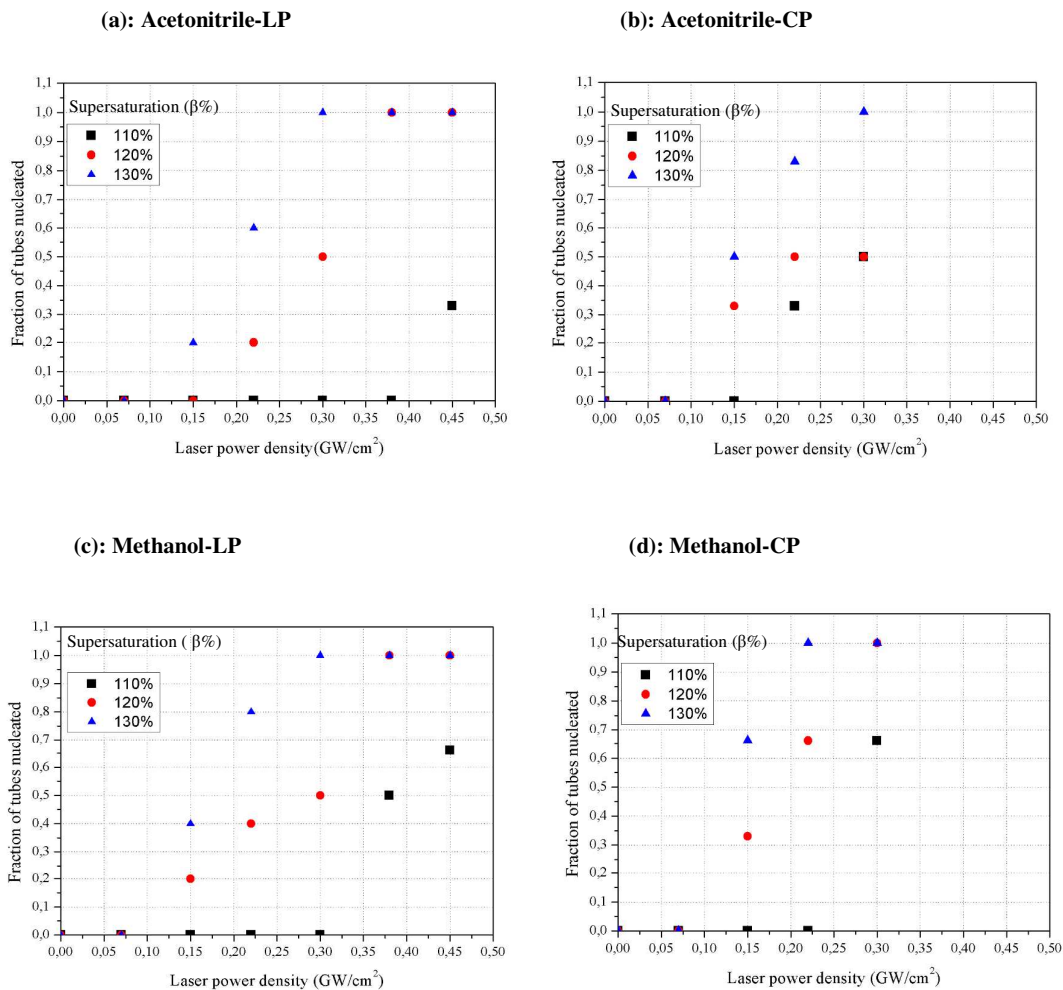


Figure 9

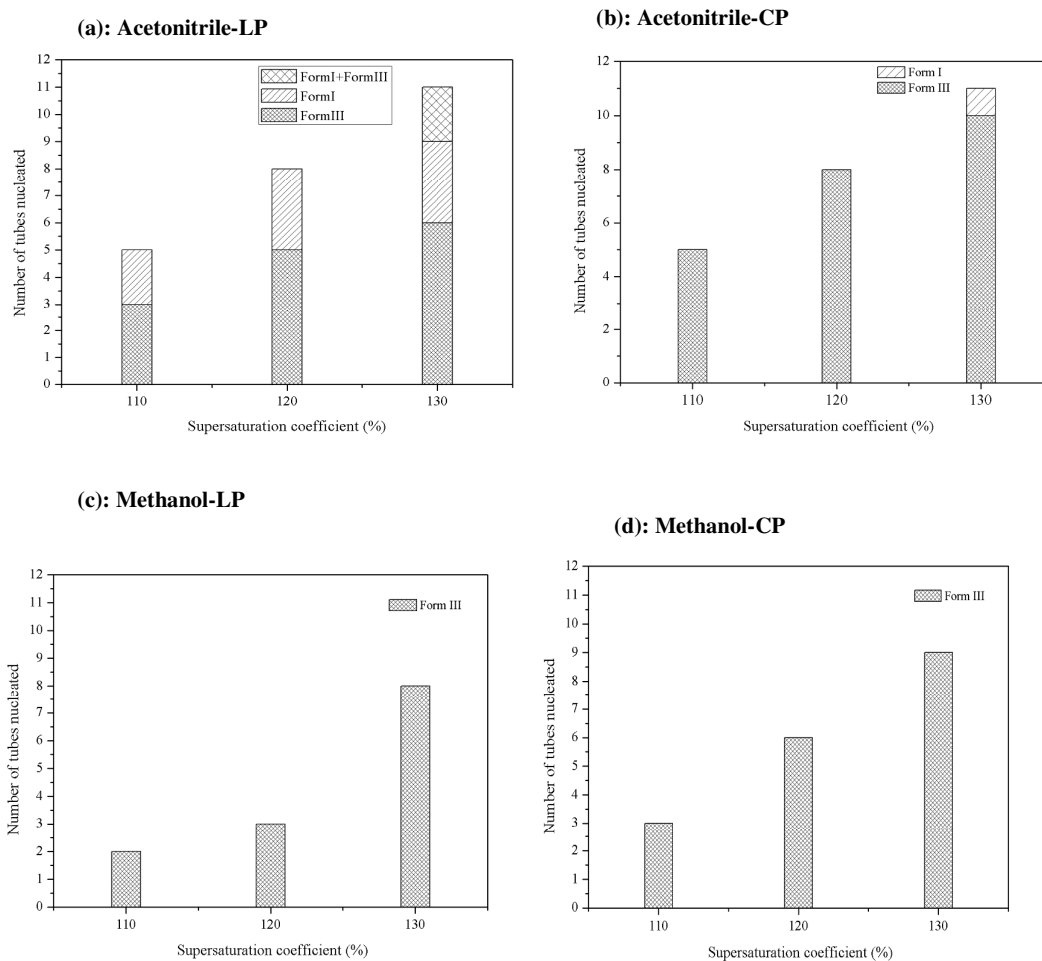


Figure 10

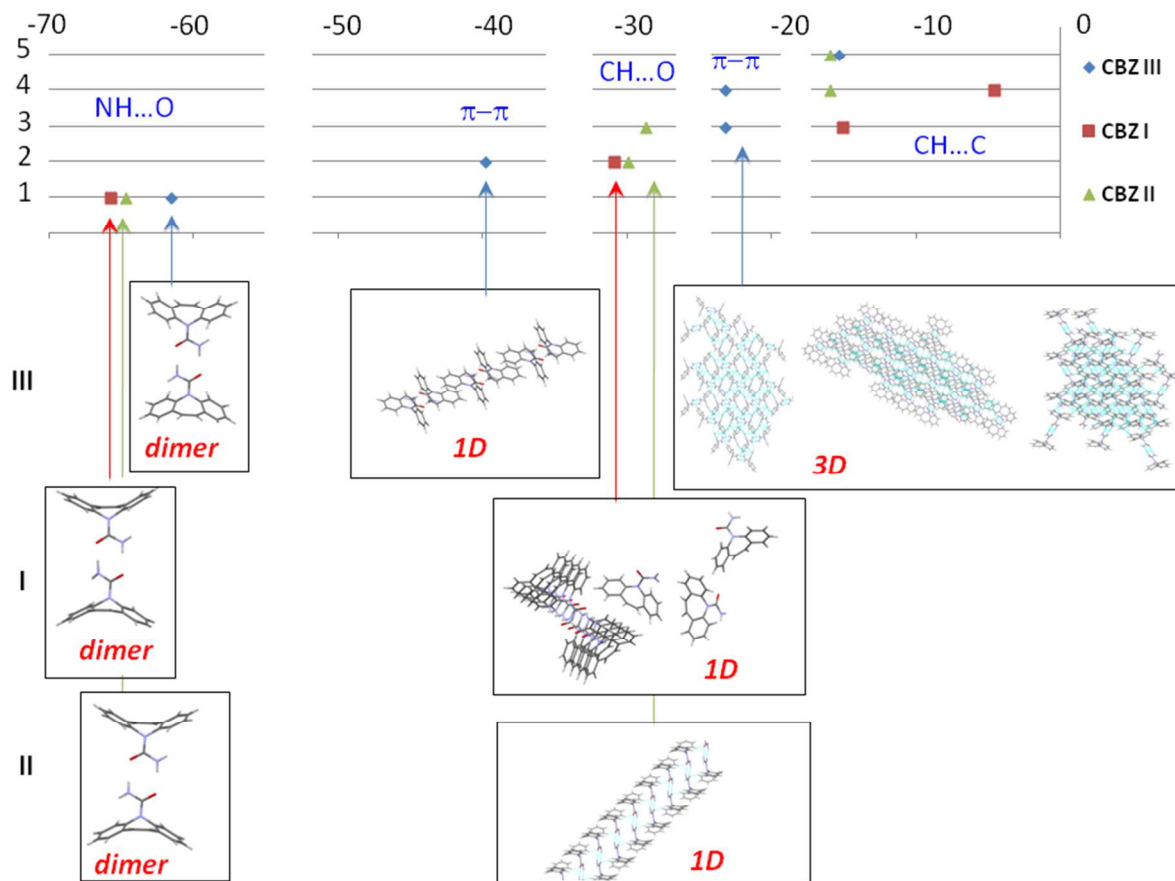
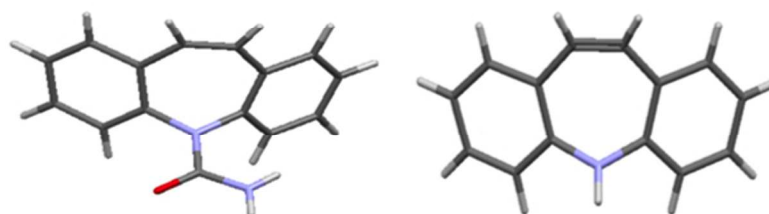


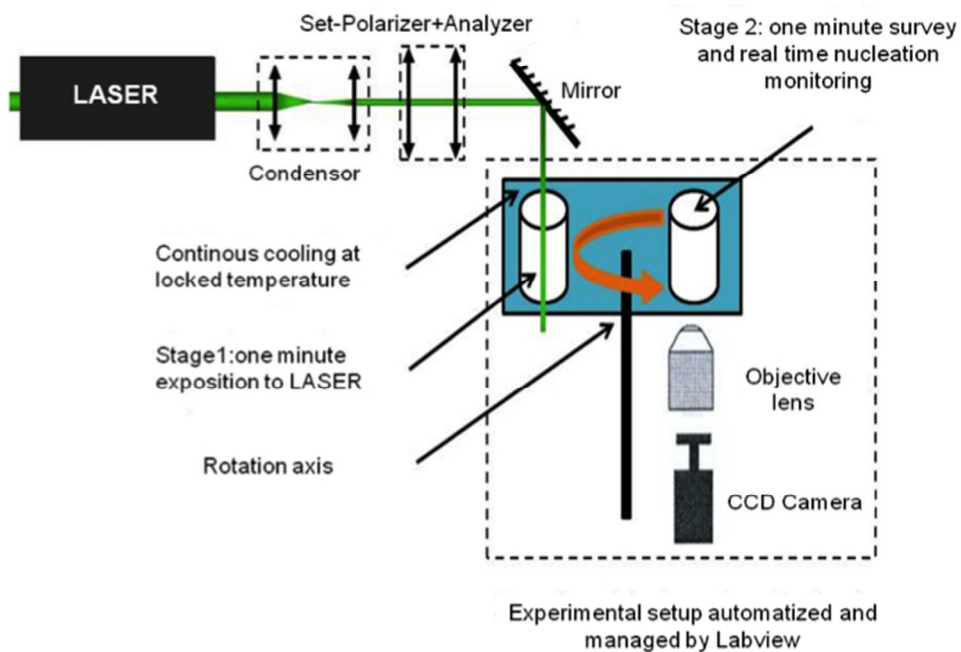
Figure 11



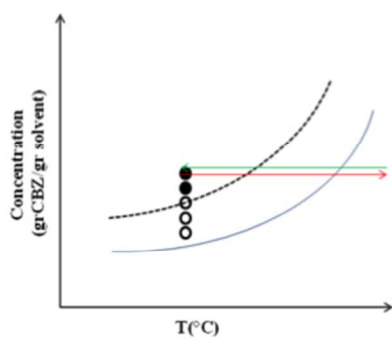
a

b

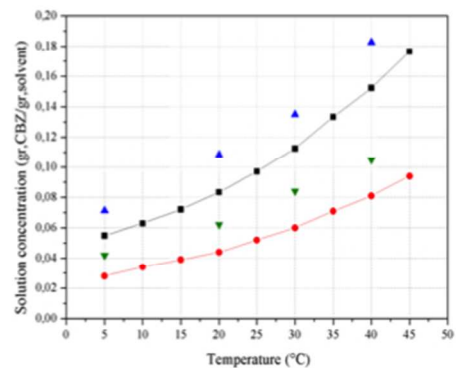
254x190mm (72 x 72 DPI)



254x190mm (72 x 72 DPI)

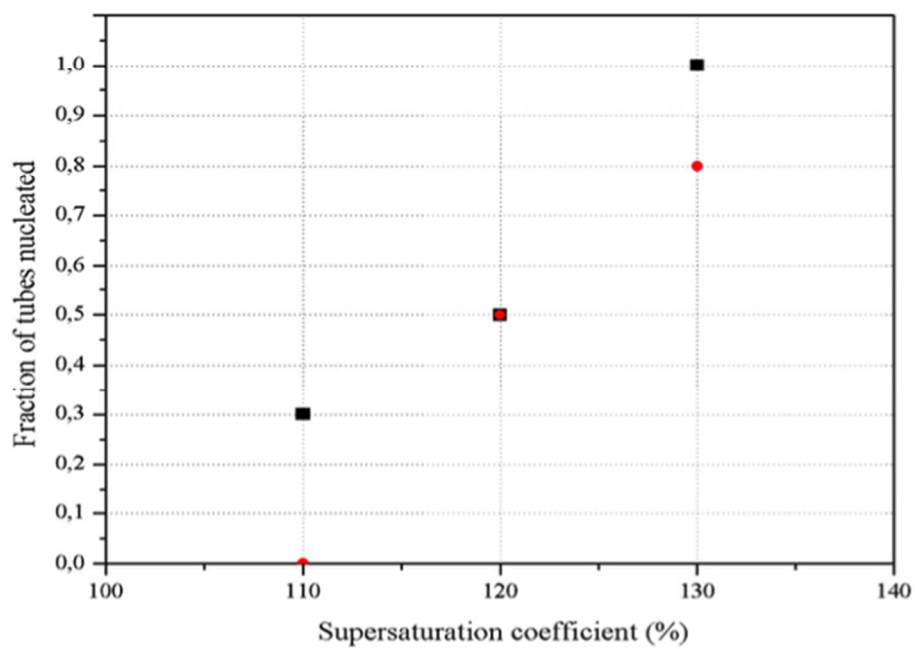


a



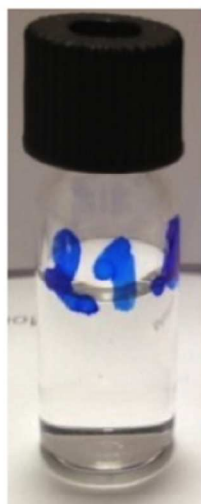
b

254x190mm (72 x 72 DPI)



254x190mm (72 x 72 DPI)

1
2
3
4
5
6
7
8
9
10
11
12
13
14
15
16
17
18
19
20
21
22
23
24
25
26
27
28
29
30
31
32
33
34
35
36
37
38
39
40
41
42
43
44
45
46
47
48
49
50
51
52
53
54
55
56
57
58
59
60



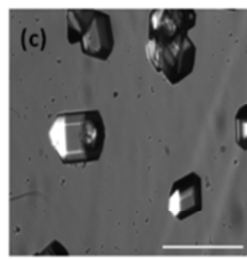
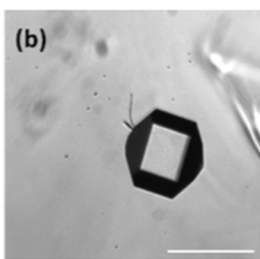
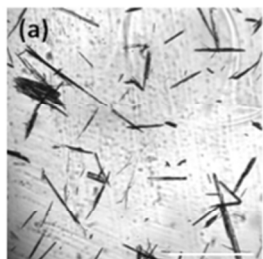
a



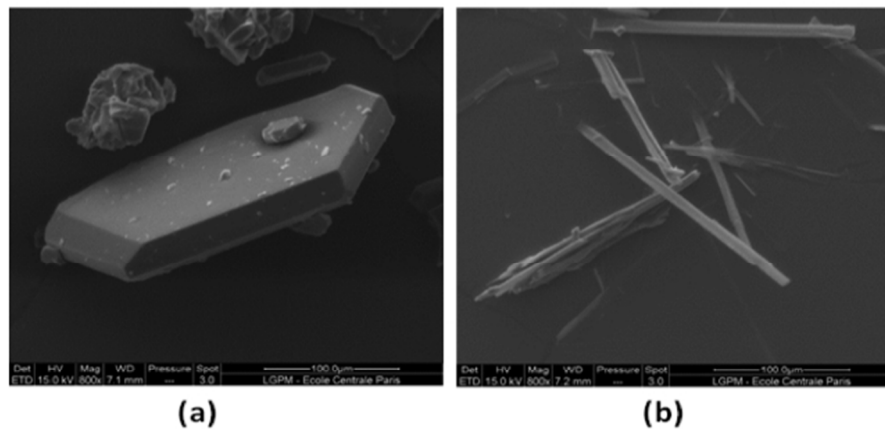
b

254x190mm (72 x 72 DPI)

1
2
3
4
5
6
7
8
9
10
11
12
13
14
15
16
17
18
19
20
21
22
23
24
25
26
27
28
29
30
31
32
33
34
35
36
37
38
39
40
41
42
43
44
45
46
47
48
49
50
51
52
53
54
55
56
57
58
59
60

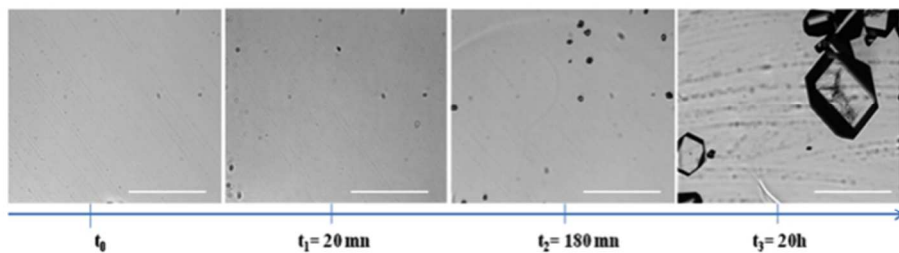


254x190mm (72 x 72 DPI)

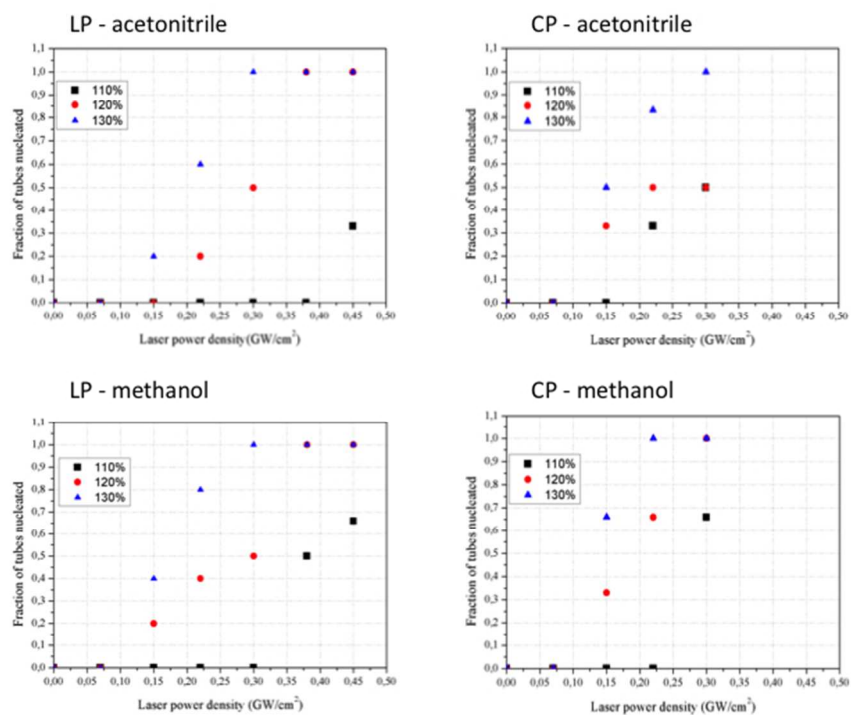


254x190mm (72 x 72 DPI)

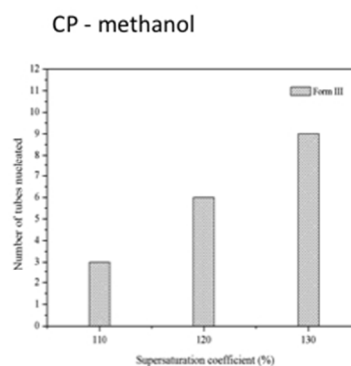
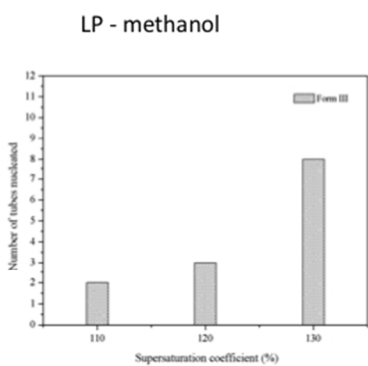
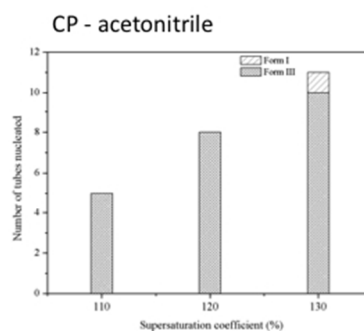
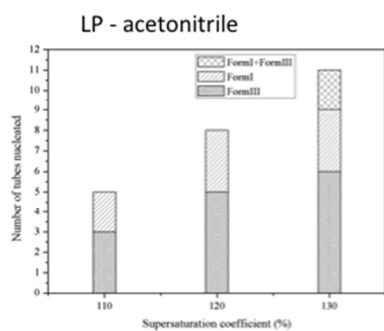
1
2
3
4
5
6
7
8
9
10
11
12
13
14
15
16
17
18
19
20
21
22
23
24
25
26
27
28
29
30
31
32
33
34
35
36
37
38
39
40
41
42
43
44
45
46
47
48
49
50
51
52
53
54
55
56
57
58
59
60



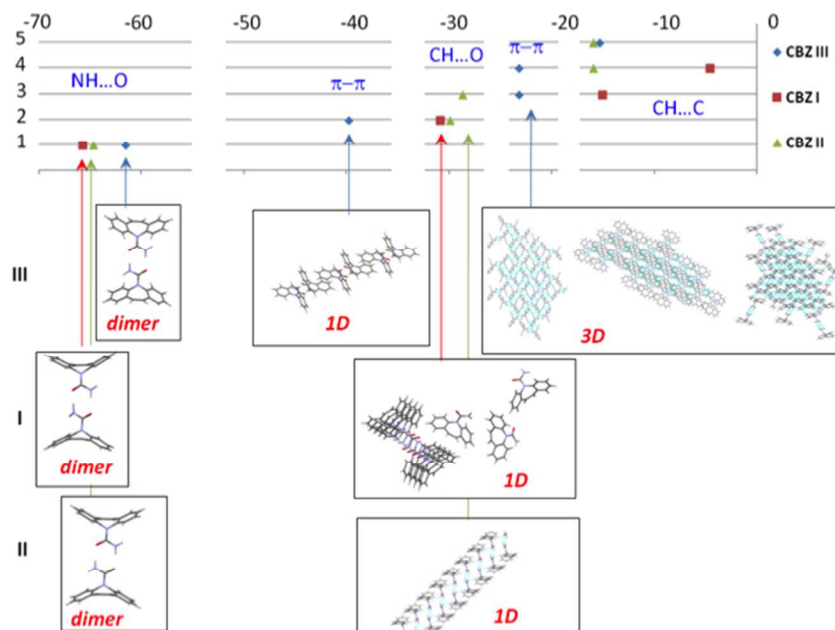
254x190mm (72 x 72 DPI)



254x190mm (72 x 72 DPI)



254x190mm (72 x 72 DPI)



254x190mm (72 x 72 DPI)